THE TECHNIQUES OF SCALING FOR HYDRAULIC PHYSICAL MODELING

by Chen, Yi-Ching*

(Introduction)

In civil engineering, hydraulic modeling has contributed significiently to design of hydraulic structure, river regulation and even basic research. Hydraulic model tests are particularly useful in the study of complex flow phenomena for which no completely satisfactory analysis is available. The basic idea of modeling refers to the possibility of investigating phenomena accurately by using relatively simple equipment and devices and by devoting comparatively little time and money.

When engineers design hydraulic structures, three ways are commonly approached: by theory; by experience; or by testing the proper model studies. Owing to lack of experience in different conditions and theoretical identification for hydraulic design, the experimental work on scale modeling is still the most efficient, and sometimes the only, method of solving the nonuniform and unsteady flow problems (Novak & Calbelka, 1981). Although sometimes hydraulic modeling is rather routine and no special skill is demanded, " hydraulic modeling is still more of an art than a science " (Shen, 1978).

Although hydraulic physical modeling is an old science, it is also important today. Now there are probably hundreds, if not thousands, of hydraulic models tests being conducted each year by various governmental agencies, universities, research institutes and private laboratories all over the world. However there are also many difficulties in modeling being necessary for researchers to solve not only in theory but also in practice.

Although physical modeling is a good way to help researchers to analyze the complex flow phenomena in hydraulic engineering, it needs accurate and efficient scaling techniques to eliminate the errors in modeling to get a perfect result and accurately simulate the prototype.

(Basic theory of dimensions)

The realm of mechanics consists of a variety of concepts such as energy, force, velocity, density, etc.. However, those quantities can be defined by means of only three basic independent entities-- length, time, and mass, i.e.

$$[a] = f(L, T, M) = L^{\alpha} T^{\beta} M^{\gamma}$$

A dimensional quantity, [a], encountered in mechanics is said to be:

(1) a geometric quantity if $\alpha=0$; $\beta=0$; $\gamma=0$
(2) a kinematic quantity if $\alpha=0$; $\beta=0$; $\gamma=0$
(3) a dynamic quantity if $\alpha=0$; $\beta=0$; $\gamma=0$

---

*Graduate student, hydraulic program, Dept. of Civil Engrg., Colorado State University.

If all the exponents are zero, i.e. $\alpha=\beta=\gamma=0$, then the unit of quantity, $[a]$, is refered to as a dimensionless quantity (Yalin, 1971 & Shen, 1978).

The possibility of the formation of a dimensionless power product out of the quantities $[a_1]$, $[a_2]$, and $[a_3]$ having the dimensions

$$[a_1] = L^{\alpha_1} T^{\beta_1} M^{\gamma_1}$$
$$[a_2] = L^{\alpha_2} T^{\beta_2} M^{\gamma_2}$$
$$[a_3] = L^{\alpha_3} T^{\beta_3} M^{\gamma_3}$$

depends on whether the determinant

$$\Delta = \begin{vmatrix} \alpha_1 & \beta_1 & \gamma_1 \\ \alpha_2 & \beta_2 & \gamma_2 \\ \alpha_3 & \beta_3 & \gamma_3 \end{vmatrix}$$

If $\Delta = 0$, then the formation of a dimensionless power product is possible, and thus the dimensions of $[a_1]$, $[a_2]$, and $[a_3]$ are dependent. Conversely, if $\Delta \neq 0$, then the dimensions of $[a_1]$, $[a_2]$, and $[a_3]$ are independent. The dimensions of quantities used in hydraulics are listed in Table 1.

Table 1. (Yalin, 1971)

Dimensional quantity	α	β	γ	Dimensional quantity	α	β	γ
Length	1	0	0	Stress (pressure)	−1	−2	1
Time	0	1	0	Density	−3	0	1
Mass	0	0	1	Specific weight	−2	−2	1
Velocity	1	−1	0	Viscosity	−1	−1	1
Acceleration	1	−2	0	Kinematic viscosity	2	−1	0
Volumetric flow rate	3	−1	0	Work (energy)	2	−2	1
Force (weight)	1	−2	1	Power	2	−3	1

(Dimensional analysis)

There are two common methods for dimensional analysis. The first one is Rayleigh's method. In 1899, Lord Reyleigh made an ingenious application of the principle of dimensional homogeneity and in his method, the quantities having different dimensions are combined as the product of powers of the independent quantities.

The other method is Buckingham's theorem(Buckingham, 1914). This theorem allows us to conclude that in any physical problem involving n variables in which there are k dimensions, the variables can be rearranged into n-k dimensionless parameters, as

$$f (A_1 , A_2 , \ldots , A_n) = 0$$

then, with k dimensions involved, it will be

$$f (\pi_1 , \pi_2 , \ldots , \pi_{n-k}) = 0 .$$

Those two methods are not too difficult, however, the most diffcult is to describe how to select the variables which are relevant to any particular phenomenon. It is due to the extremely varied nature of fluid system and complexity of flow phenomena. Sharp (1981) suggested some guidelines for solving this difficulity in very general terms.

(1) Free surface flow are mostly a gravity phenomenon for

which gravitational acceleration is important.

(2) If the flow is completely turbulent, viscous influence may be important and the coefficient of dynamic viscosity should be included.

(3) Surface tension forces are normally very small and generally are important only if the phenomenon under consideration is also small.

(4) Compressibility effects are usually negligble in model of water phenomena, except in case such as waterhammer.

(Basic theory of similarity)

Since the dimensionless quantities remain the same in all systems of fundamental units, the dimensionless quantities will not change if the system of fundemental units L', T' and M' by which they are expressed is replaced by a different system of units L", T" and M", i.e. transformation formulae, thus

$$L" = \lambda_L L'$$
$$T" = \lambda_T T'$$
$$M" = \lambda_M M'$$

where the proportionality factor λ_L , λ_T , and λ_M are some arbitary constant. This property means that the laws governing mechanical phenomena would remain exactly the same if the units L', T', and M' were to become λ_L , λ_T , and λ_M times different. There are three basic similarity systems, i.e.

(1) geometrically similar system: $\lambda_L = L"/L'$

(2) kinematically similar system: $\lambda_L = L"/L'$; $\lambda_T = T"/T'$

(3) dynamically similar system: $\lambda_L = L"/L'$; $\lambda_T = T"/T'$; $\lambda_M = M"/M'$

In hydraulic physical modeling, the system S' will be identified with the nature phenomenon or the prototype, while the system S" will be identified with its model.

Geometric similarity requires the shape of the model to be the same as that of the prototype. It is achieved by making sure that each length of the prototype is reduced by a constant facter called the scale.

Kinematic similarity requires that the shape of the streamline at any particular time is same in model and prototype. For these to be the same at the boundaries of the fluid system, it is obvious that the boundaries themselves must be similar and thus it can be seen that geometric similarity is a prerequisite of kinematic similarity.

However, those similarities are not sufficient to ensure that the motion of the fluid in model and prototype will be similar. Movement is caused by the action of forces. The relationship between motion and force requires that the force action in the model must be in the same direction as in the prototype. Furthermore, because it is the resultant of a number of forces which cause motion, the polygon of forces acting on a partical of fluid in the model must be geometrically similar to the equivalent prototype force polygon. This leads to the basic requirement for dynamic

similarity, namely that the ratio of any two forces acting in the model must be equal to the corresponding force ratio in the prototype.

(Similitude analysis)

There are two basic approaches to similitude analysis which apply the similarity theory in the derivation of function equations.

The first method makes use of the Buckingham π theorem to predict the necessary number of dimensionless parameters. These parameters are listed below in Table 2.

Table 2. (Sharp, 1981)

STANDARD DIMENSIONLESS PRODUCTS RELEVANT TO FLUID MECHANICS†

Name	*Format*	*Comment*
Froude number	$V/(gL)^{1/2}$	May also be defined as the square of this quantity. Relevant to gravity forces
Reynolds number	VL/ν	Relevant to viscous force action
Weber number	$V(\rho L/\sigma)^{1/2}$	May also be defined as the square of this quantity. Refers to the action of surface tension forces
Euler number	$\Delta p/(\rho V^2)$	Also expressed as $V/(2\Delta p/\rho)^{1/2}$. Important when pressure forces exist. Δp = pressure difference
Cauchy number	$\rho V^2/K$	Relevant to system where compressibility is important. K = bulk modulus of fluid
Mach number	V/C	Refers to compressibility effects – high-speed flow. C = local velocity of sound wave in fluid
Richardson number	$g\rho'/\rho(V')^2$	Relevant in cases where fluids mix or interact. ρ' and V' represent vertical density and velocity gradients, i.e. $\partial\rho/\partial H$ and $\partial V/\partial H$
Froude–Reynolds number	$g^{1/2}H^{3/2}/\nu$	Combined gravity and viscous effects.
Thoma number	$(p_1-p_v)/(p_2-p_1)$	A form of cavitation parameter. p_1 and p_2 are absolute pressures on the low- and high-pressure sides of a hydraulic machine. p_v is the vapour pressure of the liquid

†Except where noted the notation is as used in the main text.

The alternative method of analysis is generally less applicable but valuable in certain specific circumstances. In the case where the dependent variable is a force, it is possible to write a dimensionally homogeneous equation in which every term has dimension of force, e.g.

$$Fd = \phi (Fi, Fg, Fv)$$

which on expansion to dimensionless relationship, is

$$Fd/\rho L^2 V^2 = \phi (V/\sqrt{gL}, VL/\nu)$$

where $V/\sqrt{gL}$ is froude number and VL/ν is Reynolds nimber. In most hydraulic physical modeling, viscosity force(Fv), gravitational force(Fg) and internal force(Fi) are relevant so that some form of Froude number and Reynolds number must be important. Gravitational force is present in majority of fluid system, therefore, the flow through and over most hydraulic structures is affected by gravity. However, viscous force are important whenever the flow is not fully turbulent or where flow occurs around a submerged body.

The Froude number and Reynolds number are the most useful parameters for hydraulic physical modeling. Those

who make similitude analysis should put them in mind.

(Scaling a hydraulic model)

The fundamental scale for any hydraulic model is the geometric scale; that is the ratio of some length in the model to the corresponding length in the prototype. The choice of a suitable geometric scale depends on the type of fluid system which is to be studied and on the space available to build a model

Once the scale of the model has been fixed, the requirements for dynamic similarity may be used to determine other model scales. These are needed in order to operate the model so that it will be dynamically similar to the prototype and so that measurements made in the model may be used to determine prototype values.

The composition of invariant numbers is not restricted to the ratio of two quantities, but several quantities may also be combined into an invariant group. The invariant groups more commonly used will be derived subsequently, starting from the "Newton number". Under Newton's second motion law,

$F = m\,a$ where m is mass and a is acceleration

this equation can be assumed by the form,

$F = \rho L^2 V^2$ where ρ is density, L is length and V is velocity

By using dynamic similarity,

$Fm/Fp = \lambda_F = N$ where N is Newton number, a dimensionless invariant quantity

rearranging terms so that quantities relating to one system should figure on the same side of the equation

$$Fm/\rho mLm^2 Vm^2 = Fp/\rho pLp^2 Vp^2 = N$$

Applying to the force of gravity, $Fg = mg = \rho L^3 g$, the rearrangment of terms yields the "Froude number". Since the term of

$$\rho mLm^3 g/\rho mLm^2 Vm^2 = \rho pLp^3 g/\rho pLp^2 Vp^2$$

can be simplified as

$Vm^2/gLm = Vp^2/gLp = Fr$ (this is also a dimensionless invariant quantity)

The Newton number can be used also for deriving the Reynolds number, by taking into consideration the viscous force $Fv = \mu dV/dyA$ which can be changed form as $Fv = \rho\nu V/LL^2$. (ν is kinematic viscosity). Therefore, the terms

$$\rho m\nu mVmLm/\rho mLm^2 Vm^2 = \rho p\nu pVpLp/\rho pLp^2 Vp^2$$

can be simplified as

$VmLm/\nu m = VpLp/\nu p = Re$

and the Reynolds number is obtained.

Although scaling criteria vary depending on the particular model law, the procedure used to generate these scales dose not change. It is, therefore, sufficient to demonstrate this procedure using the two invariant quantities most appropriate to hydraulic models, i.e. Froude number and Reynolds number.

(1) When gravity forces are important, it has been shown that the Froude number, in some form, must be the same in model and prototype, i.e. $Vm/(gLm)^{1/2} = Vp/(gLp)^{1/2}$.

Assuming that the gravitational accleration is constant over the surface of the earth, rearrangment of above equations gives the velocity sacle,

$Vm/Vp = (Lm/Lp)^{1/2}$ where Lm/Lp is the geometric scale

In the same way, other scales may be derived by transforming the Froudian requirement into different forms, like that Q (discharge) is proportional to the product of velocity and area, so $V = Q/L^2$ substituting in equation of Froude similarity, $Qm/Qp = (Lm/Lp)^{5/2}$. Transformation to take account of time is made using $V \propto L/T$, so that $Tm/Tp = (Lm/Lp)^{1/2}$. For force sacle, using equation $F/\rho L^2 V^2$ as the basis of similarity,

$Fm/\rho mLm^2 Vm^2 = Fp/\rho pLp^2 Vp^2$ so that

$Fm/Fp = (\rho m/\rho p)(Lm/Lp)^2 (Vm/Vp)^2$

Assuming that the model and prototype are operated with the same fluid,i.e. $\rho m=\rho p$, and $Vm/Vp=(Lm/Lp)^{1/2}$, it lead to $Fm/Fp = (Lm/Lp)^3$.

(2) Scales for model, involving viscous forces are dependent in exactly the same manner as Froude similarity but are based on the fundamental requirement for Reynolds similarity.

$VmLm/\nu m = VpLp/\nu p$ or

$Vm/Vp = (\nu m/\nu p)(Lp/Lm)$

Following the method as in Froude similarity, the discharge, time and force sacles may be calculated as

$Qm/Qp = (\nu m/\nu p)(Lm/Lp)$

$Tm/Tp = (\nu m/\nu p)(Lm/Lp)^2$

$Fm/Fp = (\rho m/\rho p)(\nu m/\nu p)^2$

Most hydraulic models are concerned primarily with gravitational effects. Viscous forces,if relevant,are often handled by combining the model results with some empirical analytical work. However, viscous scaling is of importance in models which deal with fluids other than water and in cases such as the testing of submarines where gravity effects are absent.

(Distortion in modeling)

In a river fixed-bed model, it must be more complex because friction is of obvious importance in determining the movement of water along the channel. Thus, in addition to the gravitational force simulation required, it is necessary also ensure similarity of the frictional forces. Commonly a river model might be designed to investigate some problem over a reach of several kilometers in which depths are no more than a few meter. Therefore, a distorted scale is necessary.

Flow in open channel occurs under the influence of gravitayional forces and frictional forces, i.e. under Froude similarity and Reynolds similarity. This is drag force, Fd = Fg+Fv, influences the the flow. However, at high Reynolds number, drag force (or head loss) is independent of Reynolds number and drag force is dominated by form drag.

Similarity of friction resistence will be ensured provided the model and prototype both obey the same resistence law. The Manning's equation is probably most widely used :

$V = 1/n\ R^{2/3} S^{1/2}$ where n is Manning's coefficient

If the same law applied to model and prototype :

$Vm/Vp = (np/nm)(Rm/Rp)^{2/3}(Sm/Sp)^{1/2}$

and under Froudian similarity, Vm/Vp=(Lm/Lp) as mentioned in previous section, so that

$nm/np = (Lm/Lp)^{1/6} = (Km/Kp)^{1/6}$ where K is roughness height

Under normal condition, the roughness value in prototype is much smaller, however, after the similarity of the above equation, the roughness value in model should be much more smaller than that in prototype. It should be impossible and much difficult to simulate the roughness in model. In the same time, we also have some difficulties to construct a model. Firstly, there is a problem of measurement of depth and velocity which is very small in model. Secondly, the flow is rough turbulent in prototype. However, after the simulation, the flow in model will not be rough turbulent.

Therefore, the distorted scale model will be a good way to overcome all these difficulties. Under distorted model, the slope scale will be

$Sm/Sp = (Ym/Yp)/(Xm/Xp) = e$

so, the equation of Manning's roughness will be changed to

$nm/np = (Ym/Yp)^{1/6} e^{1/2}$

These changes solve all the problems discussed earlier. Use of a larger depth scale increase model depth, velocity and roughness value. This promotes turbulence and, at the same time, facilitates measurements.

The other point which we have to notice is to calibrate model by running it at a discharge which simulates a prototype discharge for which surface profiles have previously been recorded. Especially, from reach to reach, Manning's n will not be constant, therefore, we have to calibrate the roughness by angular pebbles, wire mesh, vertical pegs or some other method to increase or decrease the roughness in the channel of model and by trial-and-error to obtain the correct resistence.

The principle of choosing an ideal distorted sacle of a model is that the model should be as large as economically possible and the horizontal scale would normally be chosen on this basis. Roughness, turbulence and accuracy of depth measurement in the model depend on the vertical scale which must be chosen to satisfy these criteria.

The mobile-bed model certainly has the same difficulties as mentioned in fixed-bed model. Therefore, the distorted scale should be necessary also in the mobile-bed model. But, the consideration of distorted scales will be more complex in the mobile-bed model than those in the fixed-bed model. Einstein and Chien (1956) had discussed some principles about the consideration of distorted river model with movable beds. In their studies, several distortions were contemplated.

(1) If the ratio of horizontal lengths Lr is independent of hr, the model is vertically distorted.
(2) If the grain-size ratio Dr is different than both Lr and Hr, a third length scale is introduced and with it a second distortion.
(3) If the slope ratio Sr is chosen independently of Lr and hr, the model is assumed to be tilted in addition to other distortions.
(4) If the ratio of effective densities of the sediment, $(\rho s-\rho f)r$, is assumed to be different than the ratio of the fluid densities, ρfr, which is unity, there is a fourth distortion.
(5) A fifth distortion is introduced if t1r, the hydraulic-time ratio for the time values involved in the determination of velocities and sediment rates, is chosen differently from t2r, the sedimentation-time ratio of durations for individual flow condition, indicating the speed at which flow-duration curve are duplicated.
(6) A sixth distortion is a result of the impossibility of obtaining suspended-load rates in a model in the same scale at which the bed-load rates are reproduced; that is, the bed-load-rate $q_B r$ is different from the total-load-rate $q_T r$.
(7) A seventh distortion permits the ratio of settling velocities of corresponding grains, Vsr, to be different than the ratio of corresponding flow velocities.

(Scaling errors)

The model scales are based on their particuler requirement for dynamic similarity. Most are developed from the Froude number or Reynolds number. However, fluid systems are invariably subject to a number of force actions and it is not always possible to meet simultaneously all the criteria for full physical similarity. For example, if the same fluid is used in model and prototype, it is not possible to satisfy both Froude and Reynolds number criteria at the same time.

$Vm/Vp = (Lm/Lp)^{1/2}$ based on Froude number

$Vm/Vp = Lp/Lm$ based on Reynolds number

therefore, with a geometric scale of 1/100 Froudian similarity requires a velocity scale of 1/10 whereas viscous similarity requires a velocity scale of 100/1. There are different scale quantities listed below between the Froude number and Reynolds number in Table 3.

Table 3. (Ivicsics, 1980)

Quantity	Froude number basis	Reynolds number basis
Length	λ	λ
Area	λ^2	λ^2
Volume	λ^3	λ^3
Time	$\lambda^{0.5}$	λ^2
Velocity	$\lambda^{0.5}$	λ^{-1}
Acceleration	1	λ^{-3}
Force	λ^3	1

If other force actions are considered, other, different,sets of scales would be obtained. These variations in the scaling criteria show the general impracticability of constructing a model which is to model the prototype on the basis of scale chosen to suit the dominant force action and to allow the other forces to out-of-scale. This results in errors known as "scale errors".

In the other way, scale errors may also be caused by building and operating the model in such a way that forces which are unimportant in prototype become important in the model. The model is considerably smaller than prototype and it is inevitable that viscous and surface tension forces will become proportionately greater as the size of the fluid system is reduced. This cannot be corrected but it is possible, by avoiding an excessively small model, to ensure that these forces do not become of undue important .

The scale errors become even more conspicious when the processes considered, are more involved and call for the simultaneous observation of different criteria controlled by several variables. Unfortunately, during the solution of many practical problems, a great number of hydromechanical phenomena are encountered, the characteristics of which would require the application of several model laws. It is for this reason that the theory of modeling often fail to offer guidance towards the solution of the more complex problems and proves thus useless in the very case where the complexity of the problem would call mostly for a firm theoretical foundation.

(The methods of eliminating scaling errors)

As mentioned in previous section, scale errors may be small and negligible; but, under certain condition for other non-dominant forces are important and not negligible, the scale errors will induce the inaccuracy for simulating in modeling. The author will discuss some methods to eliminate or to avoid those errors.

(1) The velocity scales derived from Froude number and Reynolds number are different.

$V_m/V_p = (L_m/L_p)^{1/2}$ derived from Froude number

$V_m/V_p = L_m/L_p$ derived from Reynolds number and assumeing $\nu_m=\nu_p$

It shows, for example, that if models are tested in water ($\nu_m/\nu_p=1.0$) at a scale of 1/36, the model velocity should be 1/6 times than the expected prototype velocity; however, if the viscosity effects are important and we should consider the Reynolds similarity, the model velocity should be 36 times greater than the expected prototype velocity. It is unreasonable and impractical. If we wish the consideration of both similarities can be reached, we can deal with fluids other than water in the model. The changing of model fluid viscosity will make a consistency in both Froude and Reynolds similarity.

$V_m/V_p = (L_m/L_p)^{1/2} = (\nu_m/\nu_p)(L_p/L_m)$ then

$\nu_m/\nu_p = (L_m/L_p)^{3/2}$

Therefore, we can choose proper fluid for model to match the equation above and to get a consistency of Froude and Reynolds similarity. Sometimes, we can test the model in a wind tunnel when the ratio of kinematic viscosities between air and water is considerably less than 1.0.

(2) In some cases, we can simulate one dominant force directly in model and evaluate the other forces indirectly to get results. For example, drag force in the model, Fd, has viscous, Fv, and gravitational, Fg, components : Fd = Fv + Fg.
The gravitational component is reproduced corretly in the model but the viscous force is out-of-scale. Thus, it is not possible to determine the prototype drag force directly. Instead the viscous component of the model drag must be calculated and substracted from the measured drag to give the gravitational component. We can use the equation as below to determine the gravitational component of the prototype darg force.

$(Fg)p = (Fg)m(Lp/Lm)^3$ based on Froude similarity

The prototype viscous component can then be calculated and added to the gravitational component to give the total prototype drag. This method is based on a semi-empirical basis using equations developed from experiments to determine the frictional force caused by flow past very thin flat plates to calculate the viscous component. These calculations compensate for the scale errors induced by running the model to simulate only one of the two relevant forces.

(3) The other way which Eisner F. suggested is application of several models constructed to different scales. The phenomenon under consideration is reproduced in each model; then, the characteristic quantities are measured and the results are processed graphically or numerically to find the corresponding quantities of the full-size phenomenon by "extrapolation". We can build a model under the Froude similarity consideration and another model under the Reynolds similarity consideration. Then, by comparing and extrapolation method to find the corresponding relationship of results between those two models, we can get a better simulation of prototype. However, this method has some disadvantages. The construction fee of many models to different scales are too expensive, while measurements and observations are too time consuming. Moreover, the experimental points for a curve permitting extrapolation, if too less, may be not enough accurate to make the reliablity of the extrapolation value be poor.

(4) The fourth method to eliminate scale errors is to develope some new model laws combining the major dominant model laws,like Froude number and Reynolds

number. Starting from this principle, several new invariants have been developed with the object of obtaining better understanding with the help of models on other physical phenomena. In this section there are two new model laws are discussed:

(Conclusions)

The beginning of researching a hydraulic phenomenon is based on some basic theories of dimensions, then by means of dimensional analysis, like Rayleigh's method and Buckingham's π theorem, we can investigate the relationship of several physical quantities to combine into some invariants, like Froude number and Reynolds number. Those are the basic principles for the scaling a hydraulic model.

The most useful parameters for scaling a hydraulic model are the Froude number and Reynolds number. Those are the basic similarities for the model being dynamically similar to the prototype. For certain conditions, we should choose the dominate parameter but for some kind of conditions, like that the gravity forces and viscous forces are both important, the scaling errors will be occur because of the inconsistence of those two parameters in one model. However, we can use different fluid of different viscosity in model and in prototype to reach the consistence of Froude similarity and Reynolds similarity. The method of develop a new model law to combine the principle dominate model laws is also a good way to eliminate scaling errors.

Considering the conditions that the model may be too large under undistorted scale for the economic consideration or that the vertical dimension is too small to measure the velocity and depth in the model, the distorted scale model should be necessary, especially in river model or tidal estuary model.

The scaling techniques are the keys to the success of models. The determination of scales for a model is right or not will influence the accuracy of the simulation to the prototype. Therefore, we should choose a best scale carefully to get the best results from the model for simulating the prototype.

(Appendix I. REFERENCE)

Foster, J. E., (1975). " Physical modeling techniques used in river models," A.S.C.E. 2nd. annual symposium of the waterways, harbors, and coastel engineering, San Francisco, Vol. 1, pp 540-559.

Ivicsics, L., (1980). Hydraulic Models, Water Resources Publications, Fort Collins, Colorado.

Julien, P., (1987). Erosion and Sedimentation, Colorado State University, Fort Collins, Colorado.

Novak, P. & Cabelka, J., (1981). Model in Hydraulic Engineering, Pitman Advanced Publishing Program , Boston.

Scheuerlein, H., (1973). " Simulation of sediment transport in hydraulic models," A.I.T. international symposium on river mechanics, Bangkok, Thailand, pp 1-10.

Sharp, J. J., (1981). Hydraulic Modelling, Butterworth Publishers, Boston, Massachusetts.

Shen, H. W., (1978). Modeling of River, Water Resources Publications, Fort Collins, Colorado.

Yalin, M. S., (1971). Theory of Hydraulic Models, MacMillan Press, London & Basingstoke.

(Appendix II. NOTATION)

The following symbols are used in this report:

- e = the ratio of vertical to horizontal dimension
- Eu = Eular number
- F = force; dimension of force
- Fr = Froude number
- g = gravitational acceleration
- H = vertical dimension
- h = depth
- Ks = roughness height
- L = dimension of length; horizontal dimension
- M = dimension of mass
- N = Newton number
- n = distortion; Manning coeff.
- Q = discharge
- R = hydraulic radius
- Re = Reynolds number
- S = slope
- T = dimension of time
- t = dimension of time
- V = velocity
- X = horizontal dimension
- Y = vertical dimension
- λ = the ratio of model to prototype
- ρ = density
- γ = specific weight
- μ = dynamic viscosity
- ν = kinemic viscosity

Subscripts:

- f = fluid
- g = gravitational
- i = internal
- m = model
- p = prototype
- r = ratio
- s = partical
- v = viscous

A LOOK AT PHYSICAL HYDRAULIC MODELLING

Brian M. Bennett[1]

Abstract

The use of physical hydraulic modelling has been very important to hydraulic engineers due to the fact that it is very difficult and sometimes impossible to predict the performance of rivers that have complex geometries. This paper tries to demonstrate some of the ways to model the physical hydraulic phenomena that occurs in open channel flow and discusses some of the problems associated with physical hydraulic modelling.

Introduction

The use of scaled physical hydraulic models can be traced back to the late 19th Century when Osborne Reynolds designed and operated a tidal model of the Upper Mersey at Manchester University (Novak 1981). Since that time, there have been many research laboratories built to perform scale modelling of hydraulic phenomena. This paper will discuss the use of physical hydraulic modelling in open channel flow and some of the problems associated with their use.

Physical hydraulic models are normally utilized in open channel flow by aiding in the design and construction of some type of hydraulic structure. In the design of hydraulic structures, as with any type of design, there are three different approaches. The design can be done through the use of theory and mathematical means (i.e. mathematical modelling, design equations, etc.), the use of experience and knowledge gained from the design of similar structures, or the use of physical modelling on a proposed design and make any necessary modifications due to the model performance. The real need for the scaled hydraulic modelling is due to the fact that complicated geometries of channels and structures, non-uniform and unsteady flow, sediment motion, and other physical hydraulic phenomena make the use of theoretical equations impossible. Since it is very difficult to quantitatively measure the amount of sediment in a physical hydraulic model, sediment movement is usually done on a qualitative or comparative means. This topic will be discussed at length in the paper.

Physical hydraulic modelling can be done on a undistorted scaling or a distorted scaling. Undistorted scaling is when the horizontal scale is equal to the vertical scale and distorted is when the horizontal and vertical scales are different to allow for closer prototype conditions (hydraulic similarity) in the model. This topic will be discussed later in the paper.

---

[1]Graduate Student (Master's), Colorado State University, Fort Collins, Colorado 80523

As noted, there are many considerations when designing a physical hydraulic model. In most open channel hydraulic models the importance of the inertial and gravity forces are the most predominant forces, therefore a Froudian scaling is used. This will also be discussed at length later in the paper.

In this paper, the author will discuss a project that was modelled as a rigid boundary hydraulic model, but could have been easily done as a movable bed model. The differences will be discussed in the following chapters.

Rigid Boundary Model

The project discussed previously was a harbor on a major river in the United States that had a sedimentation problem (Abt 1988). It was decided by the experimenters and the client that a rigid boundary model would be utilized and a qualitative analysis of different river structures would be done.

The first problem that was encountered was what scale would be used, so that the area to be modelled would fit into the building where the model would be constructed. The critical prototype area that needed to be modelled was approximately two to two and one-half miles of river and approximately a mile wide at its widest point. The river mechanics flume used was approximately 40 feet by 120 feet. After some debate, a horizontal scale of 150 prototype to 1 model was chosen, which enable the modelers to model 6000 feet (~1.2 miles) by 18,000 feet (~3.4 miles) of prototype area. Now it had to be decided if the model would be an undistorted model or a distorted model.

If the model was to be a undistorted model, then the flow phenomena would predominately involve only gravity and inertia, which implies a geometrically similar model. If the model is geometrically similar then dynamic similarity is also obtained. If dynamic similarity is obtained, then quantitative results may be derived from the model performance. As soon as any other forces are important, then the results are no longer quantitative and the model be must modified (Joglekar 1957).

If the model was to be undistorted, then a Froudian scaling would be done because the flow phenomena would involve only gravity and inertial forces. It has been assumed for the model purposes that the gravitational acceleration at the prototype location and the model location are the same, as well as the specific weight of the water at both locations. These seem to be relatively good assumptions, since gravitational acceleration and specific weight of water are approximately the same for both locations, although this could be a source of small error in the final analysis. According to the Froude number, $Fr = \frac{V}{\sqrt{gh}}$, the velocity (the inertial force) is equivalent to the square root of the depth times the gravitational acceleration (the gravity force). Since the gravitational acceleration of both locations is assumed to be the same, it is not important.

Therefore, under the Froudian scaling criteria, the following scale ratios may be used (Albertson 1960):

TABLE 1

Characteristic	Dimension	Ratio	(Value)
Length	L	L	150
Area	L^2	L^2	22,500
Volume	L^3	L^3	3,375,000
Time	T	L^(1/2)	12.25
Velocity	L/T	L^(1/2)	12.25
Discharge	L^3/T	L^(5/2)	275,568
Mass	M	L^3	3,375,000
Force	ML/T^2	L^3	3,375,000
Pressure	M/LT^2	L	150
Momentum (impulse)	ML/T	L^(7/2)	41,335,139
Work (energy)	ML^2/T^2	L^4	506,250,000
Power	ML^2/T^3	L^(7/2)	41,335,139

Now it was checked to see if there is hydraulic similarity in the model versus the prototype conditions. It was known that the prototype river has turbulent conditions, therefore it can be checked to see if the model also has turbulent conditions. This parameter will be checked using the Reynolds number, assuming that the kinematic viscosity of the water at the prototype area and the model location are the same. It is also assumed that the river is wide, so that the hydraulic radius is equivalent to the depth of flow. The average velocity at pool elevation of the prototype is approximately 2 fps and the average depth is approximately 20 ft, therefore the Reynolds number for the prototype is about 1.03 x 10^6, which is well into the turbulent regime. Now the prototype values would have to be scaled down to model values. From Table 1, the velocity in the model should be approximately 0.16 fps (=2/12.25) and the depth will be approximately 0.13 ft (=20/150), which will yield a Reynolds number of about 562, which is not in the turbulent regime. Therefore, the model has introduced another force into play, the viscous force.

The model could not be constructed as an undistorted model because the quantitative results gained from the model would not have any meaning because of the criteria that only the inertial and gravitational forces were the predominant forces. Therefore, a distorted model would have to be utilized to insure that the model would have turbulent flow. The distorted model may also utilize Froudian scaling technique, but the scaling ratios would change from the Table 1 due to the introduction of a new dimension from the distortion. The Froudian scaling will still be valid due to the fact that the predominant forces will be the inertial and gravitational forces again. The viscous force will now be considered to be insignificant because the flow will be in the turbulent flow regime.

The new scaling ratios would be based on the distorted Froudian scaling parameters and are similar to those scaling ratios in Table 1. The new scaling ratios are as follows:

TABLE 2

Characteristic	Dimensions	Ratio	(Value)
Length, Horizontal	L	L	150
Length, Vertical	Y	B	50
Area, Horizontal	L^2	L^2	22,500
Area, Vertical	YL	BL	7,500
Volume	YL^2	BL^2	1,125,000
Time	T	B^(1/2)	7.07
Velocity	Y/T	B^(1/2)	7.07
Discharge	LY^2/T	LB^(3/2)	53,033
Mass	YL^2	BL^2	1,125,000
Force, Horizontal	MY/T^2	LB^2	375,000
Force, Vertical	ML/T^2	BL^2	1,125,000
Pressure, Horizontal	F/YL	B	50
Pressure, Vertical	F/L^2	B	50
Slope	Y/L	B/L	0.33
Distortion	L/Y	L/B	3

Now the amount of distortion for the model must be determined. As stated before, the Reynolds number will determine the amount of distortion. First of all, a distortion factor of 2 was tried. With a distortion factor of 2, then the vertical scale will have to be 75 prototype to 1 model. This would yield a model average velocity of 0.23 fps (=2/(75^(1/2))) and a model average depth of 0.27 ft (=20/75), thus having a model Reynolds number of approximately 1589, which is out of the laminar regime, but is still not quite in the turbulent regime. In Table 3, the analysis of the amount of distortion for the model can be seen.

TABLE 3

	Depth (ft)	Velocity (fps)	Re
Prototype	20	2	1.03 x 10^6
Undistorted	0.13	0.16	562
Distorted -			
2 (150H:75V)	0.27	0.23	1589
3 (150H:50V)	0.40	0.28	2920
4 (150H:37.5V)	0.53	0.33	4495
5 (150H:30V)	0.67	0.37	6282

From Table 3, it is shown that a distortion of 3 will give turbulent flow in the model, so that the Froudian criteria

scaling can be utilized. The scaling ratio values for a distortion of 3 are given in Table 2. This was the rigid boundary model that was finally constructed. It was used primarily for qualitative analysis of different river diversion structures to keep the sediment in motion and not let it accumulate at any point.

A discussion of the drawbacks of using a rigid boundary model will be discussed in the chapter about scaling effects and will be compared to the model using the movable bed theory.

Distorted Movable Bed

As discussed in the previous chapter, physical hydraulic models can be built with a rigid boundary or they can be built with a movable bed. Unlike the rigid boundary models, the movable bed models are always distorted to allow for better hydraulic similarity. Movable bed models are usually constructed for following the scouring and/or erosion around a hydraulic structure, whereas with a rigid boundary model this may not be accomplished.

There are two approaches to the problem of modelling movable beds. The first is using a hydraulic geometry relationships and regime theory as presented by Blench, Lacey, and a few others. Where the premise is that only three independent scales, (discharge, side factor, and bed factor), are imposable on the model; all other scales will adjust themselves. The second is using an analytical derivation of the distortions in the model, as presented by Einstein and Chien in the mid 1950's. The discussion of this paper will be limited to the latter approach (Richardson 1987).

Einstein and Chien noted that there were many distortions that could be contemplated in a movable bed model. They are:

1. If the ratio of horizontal lengths (Lr) is independent of depth (hr), the model is vertically distorted.
2. If the grain-size ratio Dr is different from both Lr and hr, a third length scale is introduced and with it a second distortion.
3. If the slope ratio Sr is chosen independent of Lr and hr, the model is assumed to be tilted in addition to the other distortions.
4. If the ratio of effective densities of the sediment $(\rho_s - \rho_f)_r$ is assumed to be different from the ratio of the fluid densities ρ_r which is unity, there is fourth distortion.
5. A fifth distortion is introduced if hydraulic-time ratio t1r for the time values involved in the determination of velocities and sediment rates is chosen different from the sedimentation-time ratio t2r of durations for individual flow conditions, indicating the speed at which flow-duration curves are duplicated.
6. A sixth distortion is a result of the impossibility of obtaining suspended load rates in a model in the same

scale at which the bed-load ratio qBr is different from the total-load-rate ratio qTr.

7. A seventh and last distortion permits the ratio of settling velocities Vs of corresponding grains to be different from the ratio of corresponding flow velocities (Einstein 1956).

The relationships between the prototype and model are to be done as ratios that satisfy the flow and sedimentation formulas. The distortions listed above will be taken into account in the ratios. The method of using these ratios is a long, tedious manipulation of numbers that utilizes the procedure of trial and error.

Einstein and Chien proposed that there would be a number of criterion that must be satisfied between the prototype and the model, they are: a friction criterion, a Froude criterion, a sediment-transport criterion, a zero sediment-load criterion, and a laminar-sublayer criterion. The friction criterion utilizes a generalized Manning's equation which is:

$$V = \frac{C\sqrt{g}}{D^{m}} S^{1/2} h^{(1/2+m)}$$

where:
- V = velocity
- C = a constant
- g = gravitational acceleration
- D = grain size
- S = slope
- h = hydraulic radius
- m = unknown superscript

As can be seen, when the unknown superscript (m) becomes equal to 1/6, then the equation becomes the Manning equation. This produces n (the Manning friction factor) to become equal to $D^{1/6}$. The generalized equation can be rewritten to be the following:

$$\frac{V}{\sqrt{R_T S\, g}} = C \left(\frac{R_T}{K_S}\right)^{m}$$

where:
- R_T = hydraulic radius with bottom width as wetted perimeter
- K_S = grain size of the bed

The values for C and m are the heart of the whole method as devised by Einstein and Chien. These values are gotten by a trial and error solution which will be discussed later in the paper (Einstein 1956).

The second criterion that must be adhered to in the method is the Froude criterion. This criterion is fundamental in open channel modelling because it balances the gravitational and inertial forces of the system. It appears that it may be possible in very deep channels to remove this criterion due to the fact that the velocity changes do not significantly change the depth and any energy losses would be lumped into the friction

criteria, but this concept has not been fully developed. Therefore, the Froude criterion is still used in this method (Einstein 1956).

The third criterion is that of the sediment-transport criterion, which stipulates that intensity of the transport and the shear for individual grain sizes must be equal in both the model and the prototype. So the key is to get the density of the fluid ρ_f equal in the model and the prototype, which usually quite easy done (Einstein 1956).

The fourth criterion is that of the zero sediment-load criterion, which is that the flow in the model and the prototype must be similar at the beginning of motion of the sediment. The key in this criterion is that the laminar-sublayer must be equivalent to the grain size of the sediment. The fifth criterion is actually a duplicate of the fourth criterion which stipulates that the laminar-sublayer must be equivalent to the grain size of the sediment (Einstein 1956).

These criterion can be set out in the following equations:

Friction $V_r^2 \; S_r^{-1} \; h_r^{-1-2m} \; D_r^{2m} \; C_r^{-2} = \Delta_v$

Froude $V_r \; h_r^{-1/2} = \Delta_F$

Sediment Transport $q_{B_r} \left(\rho_s - \rho_f \right)_r^{-3/2} \; D_r^{-3/2} = 1$

Zero Sediment Load $\left(\rho_s - \rho_f \right)_r D_r \eta_r^{-1} \; h_r^{-1} \; S_r^{-1} = 1$

Laminar-sublayer $D_r \; \eta_r^{1/2} \; h_r^{1/2} \; S_r^{1/2} = \Delta_\delta$

where: η_r = ratio of the hydraulic radius R_b' referred to the surface drag to the entire radius R_T

There also some other equations that are used in describing the modelling laws. One of them is the relationship between the total load q_T and the bed load q_B. The average ratio of the two ratios is q_{T_r}/q_{B_r}, which is termed as the variable B. Another equation is the hydraulic time t_1, which is described as the amount of time which a water particle takes to move with V velocity over a distance L . Another variable is the t_2 , which is the duration of the individual flows and simulates the hydrograph which is imposed on the model. Another factor which may be introduced into the model is the tilting of the model. Normally there is not a need for tilting in a model, but if there is a need it can be handled in this method (Einstein 1956).

Out of all the prototype to model relationships, there are thirteen ratios which can describe the nine independent equations derived from the above criterion and relationships. Ten of these ratios are independent, while three are dependent. As stated previously, these equations can be solved only by trial and error

solution. The method can be done in one of three different ways, which are:

1. Select the horizontal scale L_r freely.
2. Select the vertical scale h_r freely.
3. Select the density of the model sediment freely.

The method must first start with having a lot of data of the friction conditions of the prototype river. A graph (on log-log) of $(R_T S\ g)/V^2$ versus R_T/K_s can then be produced. From this graph, the C_p and m values of the prototype conditions may be found. Now similarly, a graph for the model conditions must be generated on a trial and error basis and the C_m value can be calculated. It is important to remember for the first approximation that the m value is to be the same for both the prototype graph and the model graph. After this is accomplished, then continue by selecting which scale (L_r, h_r , $(\rho_s - \rho_f)_r$) will be taken as the free parameter. It is usually customary to chose the L_r scale because of model construction space. The other variables can be solved by using the charts listed in Table 4. If there is not agreement with some of the assumptions used to devise the model graph, then another iteration must be done until the assumptions and the solved variables are in agreement. For a better understanding of the method, it is advised that the reader refer to the original paper by Einstein and Chien(Einstein 1956).

For the example listed in the preceding chapter, there was not enough field information taken for an detailed analysis using Einstein and Chien's method of distorted modelling with a movable bed.

Scale Effects and Model Comparisons

It can be seen that the rigid boundary model cannot give an accurate account of where scour/erosion and deposition may occur, but it can be used as an indicator for sediment movement. In a movable bed model, it can be seen where the scour/erosion and deposition is occurring, but it is very difficult to quantify this phenomena. The reason for selecting a certain model is the objectives that the model are supposed to achieve. For example, if the exact location of the scour is not important, whereas the water levels are very important, then a rigid boundary model will fit the description. But if the model is of structure that depends on where the scour is occurring, such as a bridge pier, then a movable bed is probably the method to use. It should be reminded that a rigid boundary model is easier to construct, but has its obvious drawbacks, whereas the movable bed model also has some limitations in its use. The movable bed model also is a more laborious task to design.

One scaling effect of modelling is that there is a potential for an excessive frictional loss in a geometrically similar model. This usually means in a rigid boundary model that the surface of the model should be very smooth as compared to the

TABLE 4.—Model Ratios for Open-Channel Flows with Sediment Motion*

Symbol	h_r	L_r	$(\rho_s - \rho_f)_r$	C_r	v_r	B	Δ_F	Δ_S	Δ_N	Δ_o
(a) Depth Ratio, h_r, Chosen										
L_r	$\frac{4m+1}{m+1}$	...	...	$\frac{2}{m+1}$	$\frac{m}{m+1}$	...	$\frac{-2}{m+1}$	$\frac{-2m}{m+1}$	1	$\frac{1}{m+1}$
V_r	1	...	...	...	...	...	1	...	...	...
S_r	$\frac{-3m}{m+1}$	...	...	$\frac{-2}{m+1}$	$\frac{-m}{m+1}$	...	$\frac{2}{m+1}$	$\frac{2m}{m+1}$	...	$\frac{-1}{m+1}$
D_r	$\frac{2m-1}{2(m+1)}$	...	...	$\frac{1}{m+1}$	$\frac{-1}{2(m+1)}$	...	$\frac{-1}{m+1}$	$\frac{1}{m+1}$	...	$\frac{1}{2(m+1)}$
$(\rho_s - \rho_f)_r$	$\frac{3(1-2m)}{2(m+1)}$	...	...	$\frac{-3}{m+1}$	$\frac{3}{2(m+1)}$	...	$\frac{3}{m+1}$	$\frac{2m-1}{m+1}$	...	$\frac{-3}{2(m+1)}$
q_B	$\frac{3(1-2m)}{2(m+1)}$	...	...	$\frac{-3}{m+1}$	$\frac{3}{2(m+1)}$	...	$\frac{3}{m+1}$	$\frac{3m}{m+1}$	...	$\frac{-3}{2(m+1)}$
q_{Sr}	$\frac{3(1-2m)}{2(m+1)}$	...	...	$\frac{-3}{m+1}$	$\frac{3}{2(m+1)}$	1	$\frac{3}{m+1}$	$\frac{3m}{m+1}$	...	$\frac{-3}{2(m+1)}$
t_{sr}	$\frac{7m+1}{2(m+1)}$	...	...	$\frac{2}{m+1}$	$\frac{m}{m+1}$	...	$\frac{-(m+3)}{m+1}$	$\frac{-2m}{m+1}$	1	$\frac{1}{m+1}$
t_{hr}	$\frac{5m+2}{m+1}$	...	...	$\frac{2}{m+1}$	$\frac{m}{m+1}$	-1	$\frac{-2}{m+1}$	$\frac{-(3m+1)}{m+1}$	1	$\frac{1}{m+1}$
(b) Length Ratio, L_r, Chosen										
h_r	...	$\frac{m+1}{4m+1}$	...	$\frac{-2}{4m+1}$	$\frac{-m}{4m+1}$	...	$\frac{2}{4m+1}$	$\frac{2m}{4m+1}$	$\frac{-(m+1)}{4m+1}$	$\frac{-1}{4m+1}$
V_r	...	$\frac{m+1}{2(4m+1)}$	...	$\frac{-1}{4m+1}$	$\frac{-m}{2(4m+1)}$	...	$\frac{2(2m+1)}{4m+1}$	$\frac{m}{4m+1}$	$\frac{-(m+1)}{2(4m+1)}$	$\frac{-1}{2(4m+1)}$
S_r	...	$\frac{-3m}{4m+1}$	...	$\frac{-2}{4m+1}$	$\frac{-m}{4m+1}$	...	$\frac{2}{4m+1}$	$\frac{2m}{4m+1}$	$\frac{3m}{4m+1}$	$\frac{-1}{4m+1}$
D_r	...	$\frac{2m-1}{2(4m+1)}$	...	$\frac{2}{4m+1}$	$\frac{-(2m+1)}{2(4m+1)}$	...	$\frac{-2}{4m+1}$	$\frac{2m+1}{4m+1}$	$\frac{1-2m}{2(4m+1)}$	$\frac{1}{4m+1}$
$(\rho_s - \rho_f)_r$	...	$\frac{3(1-2m)}{2(4m+1)}$	...	$\frac{-6}{4m+1}$	$\frac{3(2m+1)}{2(4m+1)}$	...	$\frac{6}{4m+1}$	$\frac{2m-1}{4m+1}$	$\frac{3(2m-1)}{2(4m+1)}$	$\frac{-3}{4m+1}$
q_{Br}	...	$\frac{3(1-2m)}{2(4m+1)}$	...	$\frac{-6}{4m+1}$	$\frac{3(2m+1)}{2(4m+1)}$	...	$\frac{6}{4m+1}$	$\frac{6m}{4m+1}$	$\frac{3(2m-1)}{2(4m+1)}$	$\frac{-3}{4m+1}$
q_{Tr}	...	$\frac{3(1-2m)}{2(4m+1)}$	...	$\frac{-6}{4m+1}$	$\frac{3(2m+1)}{2(4m+1)}$	1	$\frac{6}{4m+1}$	$\frac{6m}{4m+1}$	$\frac{3(2m-1)}{2(4m+1)}$	$\frac{-3}{4m+1}$
t_{sr}	...	$\frac{7m+1}{2(4m+1)}$	...	$\frac{1}{4m+1}$	$\frac{m}{2(4m+1)}$	...	$\frac{-2(2m+1)}{4m+1}$	$\frac{-m}{4m+1}$	$\frac{m+1}{2(4m+1)}$	$\frac{1}{2(4m+1)}$
t_{hr}	...	$\frac{5m+2}{4m+1}$	...	$\frac{-2}{4m+1}$	$\frac{-m}{4m+1}$	-1	$\frac{2}{4m+1}$	$\frac{-(2m+1)}{4m+1}$	$\frac{-(m+1)}{4m+1}$	$\frac{-1}{4m+1}$
(c) Sediment-Density Ratio, $(\rho_s - \rho_f)_r$, Chosen										
L_r	...	...	$\frac{-2(4m+1)}{3(2m-1)}$	$\frac{-4}{3m-1}$	$\frac{2m+1}{2m-1}$	...	$\frac{4}{2m-1}$	$\frac{2}{3}$	1	$\frac{-2}{2m-1}$
h_r	...	...	$\frac{-2(m+1)}{3(2m-1)}$	$\frac{-2}{2m-1}$	$\frac{1}{2m-1}$	...	$\frac{2}{2m-1}$	$\frac{2}{3}$	...	$\frac{-1}{2m-1}$
V_r	...	...	$\frac{-(m+1)}{3(2m-1)}$	$\frac{-1}{2m-1}$	$\frac{1}{2(2m-1)}$	...	$\frac{2m}{2m-1}$	$\frac{1}{3}$	...	$\frac{-1}{2(2m-1)}$
S_r	...	...	$\frac{2m}{2m-1}$	$\frac{2}{2m-1}$	$\frac{-2m}{2m-1}$	...	$\frac{-2}{2m-1}$	...	...	$\frac{1}{2m-1}$
D_r	...	...	$\frac{-1}{3}$	...	...	...	...	$\frac{2}{3}$	...	...
q_{Br}	...	...	1	...	...	...	...	1	...	...
q_{Tr}	...	...	1	...	...	1	...	1	...	...
t_{sr}	...	...	$\frac{-(7m+1)}{3(2m-1)}$	$\frac{-3}{2m-1}$	$\frac{4m+1}{2(2m-1)}$	...	$\frac{2(2-m)}{2m-1}$	$\frac{1}{3}$	1	$\frac{-3}{2(2m-1)}$
t_{hr}	...	...	$\frac{-2(5m+2)}{3(2m-1)}$	$\frac{-6}{2m-1}$	$\frac{2(m+1)}{2m-1}$	-1	$\frac{6}{2m-1}$	$\frac{1}{3}$	1	$\frac{-3}{2m-1}$

* Solution with known effects of omitting Eqs. 2, 6, 11, and 16.

prototype (Joglekar 1957). If it is found that the frictional loss are less than that of the prototype, it is always easier to add friction into the model by artificial means (i.e. adding plastic roughness to the borders to simulate tree growth, adding little blocks in flood plains to simulate a greater Manning's n, etc.).

It is possible to have a side effect occur in part-width models of structures, such as weirs or bridge piers. This can cause a surface drag on the side boundaries that are not present in the prototype. This scale effect is very noticeable in narrow flume studies. It may also be possible to have to reduce the number of piers in a model due to the vertical exaggeration in distorted model scaling. The horizontal contraction may form separation points larger than that of the prototype causing dissimilar flows. It is also possible to get an excessive scouring around the piers due to the vertical exaggeration. This problem may be solved by dividing the number of piers by the vertical exaggeration of the model. An important aspect to remember is to have the even number of piers in the model, if there is an even number in the prototype and the same goes for an odd number of piers (Joglekar 1957).

In the Einstein and Chien method of movable bed modelling there are some reasons for loss of similarity between the prototype and the model. One of the major reasons is that the value of m (unknown superscript used in describing ratios) is not always the same for both the model and prototype over a large of flows. It is then suggested that the deviation be permitted to occur at the less important flows. Also if the flow is to occur in more than one channel, then the prediction of the friction equation is even more difficult, thus producing a large area for similarity to be reduced (Einstein 1956).

Another problem that could arise is the use of the time ratio for routing the flood through the model. The bed-load rates must be similar in the prototype and the model to produce similar bedforms. The bed-load rate and the total-load rate, which is derived from the hydrograph, changes with time due to the changes of stage, thus requiring a sliding time scale when the discharge range is wide. Another related problem is that of the introduction of wash load. This method does not account for deposition of sediment in low velocity zones as it is now. The method must be modified to incorporate this phase of sedimentation (Einstein 1956).

To check some of the values of different parameters with different scaling methods, the author will use a set of prototype conditions used in Einstein and Chien's paper against the undistorted and distorted values that can be generated using Table 1 and 2 of this paper and the values generated using the example as presented in Einstein and Chien's paper. The Lr was fixed at 150:1 and the C ,m, and η_r values used in the Einstein and Chien calculations are 0.902, 0.145, and 1 respectively.

TABLE 5

	Prototype	Undistorted Model	Distorted(3) Model	Einstein Model
L(ft)	150	1	1	1
Q(cfs)	35,700	0.130	0.673	0.867
V(fps)	11.30	0.92	1.60	1.74
h(ft)	4.34	0.029	0.087	0.103
t(sec)	10	0.816	1.41	0.433
S(-)	0.00105	0.00105	0.00315	0.00372

It is noted that using different scaling criteria can really change the parameter values in the model, but the results of the model should all come out to the approximately the same values, assuming that all of the scaling criteria of all the different methods have been achieved.

Summary

The most important aspect of physical hydraulic modelling is to verify the model with the prototype. After the construction of the model is complete, then a calibration of the model must be done to insure that the model is giving accurate results. Sometimes this verification process can be very long and tedious, but it is the only way insure the model is operating properly. It can be seen that the model is based upon the information obtained from the field, so the more accurate the field data, then the more accurate the model that can be reproduced.

As discussed previously, the type of physical hydraulic model used depends on the objectives of the model in the first place. If water levels, lines of flow, certain types of structural improvements are the objective of the study, then a rigid boundary model is probably the best procedure to use. If the experimenter is interested in scouring, erosion, and deposition of a river, then the logical choice is that a movable bed should be utilized. All in all, physical modelling is usually the best route to go when the geometries of the river are so complex or the cost of building a prototype that has never been built before are excessive.

Bibliography

Abt, S.R., Bennett, B.M., and Wittler, R.J.; "Clark Maritime Centre Model Study"; Colorado State University Client Report; March, 1988

Albertson, M.L., Barton, J.R., and Simons, D.B.; "Fluid Mechanics for Engineers"; Prentice-Hall, Inc., New York, New York; 1960

ASCE Task Committee on Glossary of Hydraulic Modeling Terms; "Modeling Hydraulic Phenomena: A Glossary of Terms"; ASCE Hydraulics Journal; July, 1982

Bogardi, J.; "Sediment Transport In Alluvial Streams"; Akademiai, Budapest; 1974

Einstein, H.A., and Chien, N.; "Similarity of Distorted River Models with Movable Bed"; ASCE Transaction Vol. 121; 1956

Joglekar, D.V., Gole, C.V., and Chitale, S.V.; "Scale Effects in Hydraulic Research"; IAHR 7th Gen. Meeting Vol. I (A4); 1957

Novak, P., and Cabelka, J.; "Models in Hydraulic Engineering: Physical Principles and Design Applications"; Pitman Publishing Inc.; 1981

Richardson, E.V., Simons, D.B., and Julien, P.Y.; "Highways in the River Environment"; U.S. Dept. of Transportation; January, 1987

HINGE POOL EFFECTS ON SEDIMENT TRANSPORT

By Basil K. Arthur

ABSTRACT

Hinge pool operation on low lift locks and dams are normally used to minimize damage from flooding of adjacent lands at higher discharges. The effect of hinge pool operation on sediment transport will be evaluated by use of HEC-6, and transport capacity will be evaluated by two different sediment transport equations. Hinge pool increases the water surface slope and therefore sediment transport will be increased.

INTRODUCTION

The stream chosen to model is part of the Red River which flows from Daingerfield, Texas joining the Black River becoming the Atchafalaya River in the southern part of Louisiana. The model covers a reach from Shreveport, Louisiana to river mile 199 (Post Project mileage) which is just north of Howard, Louisiana.

This reach was chosen because of available data. A sediment rating curve was available at Shreveport which will be used as the upstream boundary condition and a tailwater rating curve was available below the proposed site of Lock and Dam No. 5.

Cross-sectional geometry was obtained from the Vicksburg District Corp of Engineers.

DISCUSSION

HINGE POOL

At low level discharges, normal pool elevations are almost horizontal and at an elevation equal to or above the natural low-water stage at the upper end of the pool. As discharge increases the pool elevation is approximately constant at the downstream end while velocities rise. (Peterson) See Figure 1.

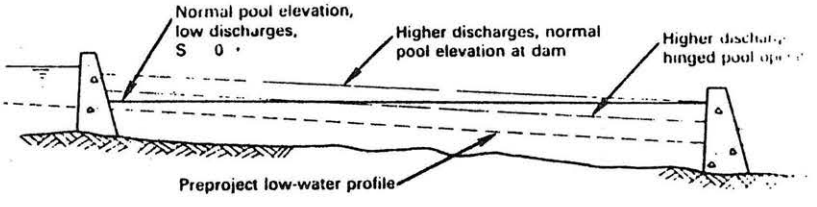

Effect of pool operation on water surface elevations

Figure 1

When the discharge is sufficient to cause stages to rise at the upper end of the pool, the additional depth is not required to maintain navigation depths and the lower pool can be lowered. The lowering of the downstream water surface increases the velocities in the lower end of the pool and increases the water surface slope over the entire pool length.

HEC-6 MODEL DESCRIPTION

This model is a simulation program designed to analyze scour and deposition by modeling the interaction between sediment material forming a stream's boundary and the hydraulics of flow.

This program is a one-dimensional steady flow model with no provision for simulating meander development, or lateral distribution of sediment load aross the cross section. Cross sections are divided into two parts, the moveable bed and the fixed bed. The entire moveable bed section is moved vertically up and down. Bed forms are not simulated except that n-values can be a function of discharge which directly provides consideration of bed forms. Secondary currents and density currents are not accounted.

Input Data Summary

Geometric Data. This section includes cross sections, n-values and reach length, which exist at the beginning of the study as would be needed for water surface profile calculations. The depth of bed sediment material and the moveable portion of each cross section are also established within this section. See Figure 2.

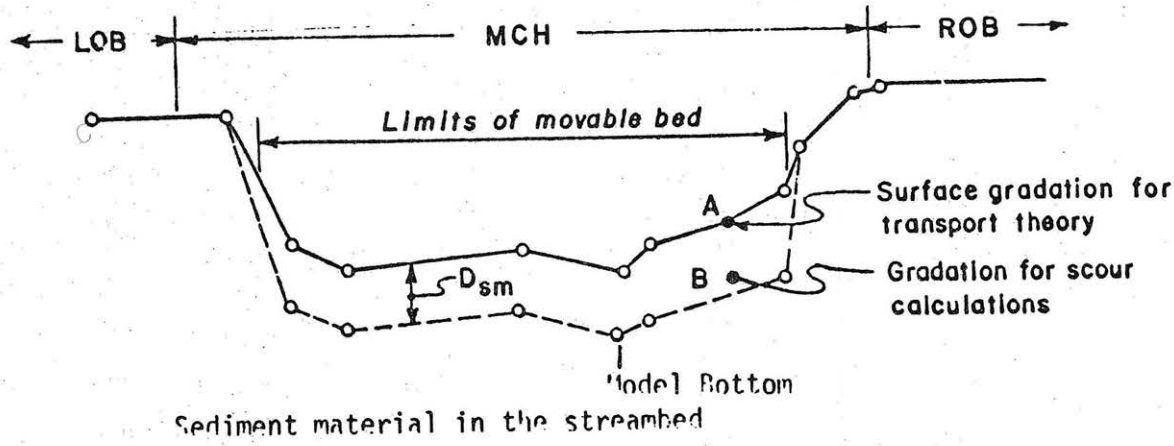

Figure 2

Sediment Data. This section contains information about the inflow sediment load, gradation of material found in the stream bed and information about fluid properties and sediment properties. If the inflowing sediment load is essentially one grain size, it can be classified for the computer program by identifying it as a sand, silt or clay. But, if the inflowing load is composed of a range of sizes, it is desirable to further subdivide the sediment load (see Figure 3). This data is normally the upstream boundary condition.

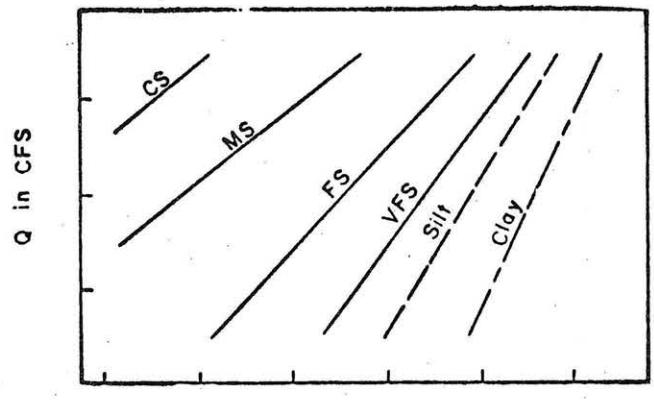

Water-sediment inflow relationship

Figure 3

Operating and Hydrologic Data. The operation is a functional relationship between starting water surface, flow and time. Hydrologic data contains water discharge, water temperatures and flow duration. Because both sediment transport and hydraulics of flow are nonlinear functions of water discharge, a continuous simulation of water discharge is needed and normally a discharge hydrograph is used (see Figure 4 on next page). The program treats a continuous hydrograph as a sequence of discrete steady flow events, each having a specified duration in days. This section is normally referred to as a downstream boundary condition.

MODEL INPUT

Geometric Data. Cross section data was obtained from the Vicksburg District Corp of Engineers. The cross sectional geometry was taken from a HEC-2 deck, which was calabrated to existing stage and discharge records. The amount of channel that was considered to be the moveable bed section was taken from water surface profiles for flows between 60,000 and 130,000 cfs. These values were chosen due to the hinge starting at 60,000 cfs

and the upper limit was rarely exceeded in the typical hydrograph.

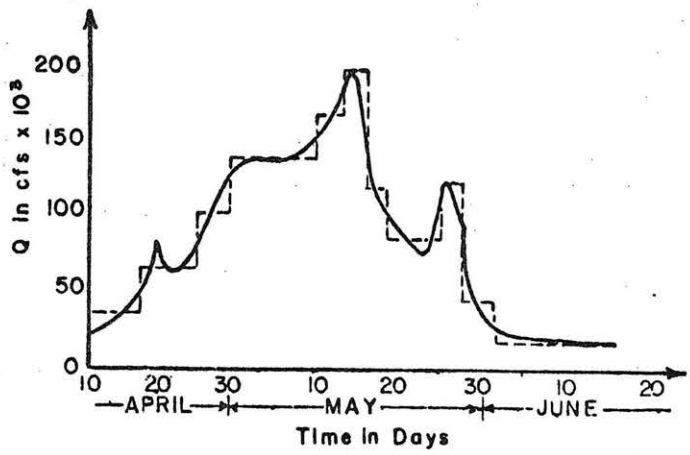

Water discharge hydrograph

Figure 4

Operating and Hydrologic Data. Navigation depth for Pool 5 can be maintained starting around 60,000 cfs flow and the pool can be lowered 1 foot for each additional 4000 cfs of flow up to 80,000 cfs (elevation 140) for a hinge of 5 feet and can be maintained at elevation 140 up to 100,000 cfs of flow. The flow will follow the tailwater to a flow of 141,000 cfs of flow. (Corp Design Memorandum) See Figure 5.

Using the tailwater rating curve and the headwater rating curve (with or without hinge) one could determine the approximate water surface elevation with varying flows.

Water year 1972 was selected as a typical hydrograph for the model. The hydrograph was selected because it peaked in the spring months and peaked in the late fall or early winter with low stage during summer and early fall.

Sediment Data. An upstream boundary condition is required for the HEC-6 model. A sediment rating curve was available at Shreveport, Louisiana. The total load versus discharge is shown in Figure 6 and the load by grain size is shown in Figure 7. The program requires the sediment rating curve to be broken in size fractions and existing data was used. The grain size ranged from a very fine sand to coarse sand with little or no clay. Approximately 80 percent of the sediment was very fine sand and fine sand.

Sediment Transport. Toffalelti's application of Einstein's bed load function was used to compare transport rates, water surface elevation, trap efficiency, and scour or deposition along the channel. (Toffaleti, 1966) The calculations were accomplished using the HEC-6 model on a personalized computer (PC). The model

shows that hinging the pool decreased the trap efficiency from 84% without hinge to 55% with hinge (about 30%).

As expected, hinging affected the water surface from 5 feet at the lower end of the model reach to approximately 1 foot at the upper end of the model reach as shown in Figure 8.

The channel cross sections indicate deposition at nearly all sections and ranged from 2 feet to 7 feet of deposition. The hinged pool run shows an average of 1 foot less deposition through the entire channel reach. See Figure 9.

Using Yang's streampower equation, the model was run again with and without hinge pool.(HEC-6) Yang's equation computed a trap efficiency 98% without hinge and 90% with hinge pool. The thalwegs show significantly more deposition in the upper half of the river reach and less deposition in the lower half when using Yang's (see Figure 10). When comparing Yang's hinge versus Toffaleti's hinge, more deposition occured 3/4 way through the pool from the upper end to lower end. Yang's method also indicated an increase in water surface for the same flow at the upper end of the pool and shows little or no effect in the lower portions.

The hydrograph used in this model was a 1 year duration and the maxium flow was 145,000 cfs (see Figure 11). When the sediment rating curve is evaluated the maximum flow is 250,000 cfs and it is apparent that the maximum historical flows on the river were not met. This indicates that a much longer duration of flow (50 years of record) needs to be evaluated in the model to make an adequate decision of sediment transport within this reach of river.

Hinge pooling generally tended to increase sediment transport with both methods.

CONCLUSION

1. The method chosen to evaluate sediment transport will significantly affect to what degree hinge pool can effect sediment transport.
2. The method (equation) used for sediment transport must be matched to the sediment type and amount.
3. Hinging the pool normally showed an increase in sediment transport.
4. Any sediment transport equation needs considerable verification before being used with a model.

REFERENCES

1. Design Memorandum No. 34 (Revised), "Hydrology and Hydraulics Design Lock and Dam No.5", U.S. Army Engineering District, Vicksburg, Mississippi.

2. HEC-6 Manual, "Scour and Deposition in Rivers and Reservoirs", U.S. Army Corps of Engineers, March 1977.

3. Peterson, Margaret S., River Engineering, Prentice-Hall, New Jersey, 1986, pp 322.

4. Toffaleti, F.B., "A procedure for computation of total River Sand Discharge and Detailed Distribution, Bed to Surface", Committe on Channel Stabilization, U.S. Army Corp of Engineers, November 1966.

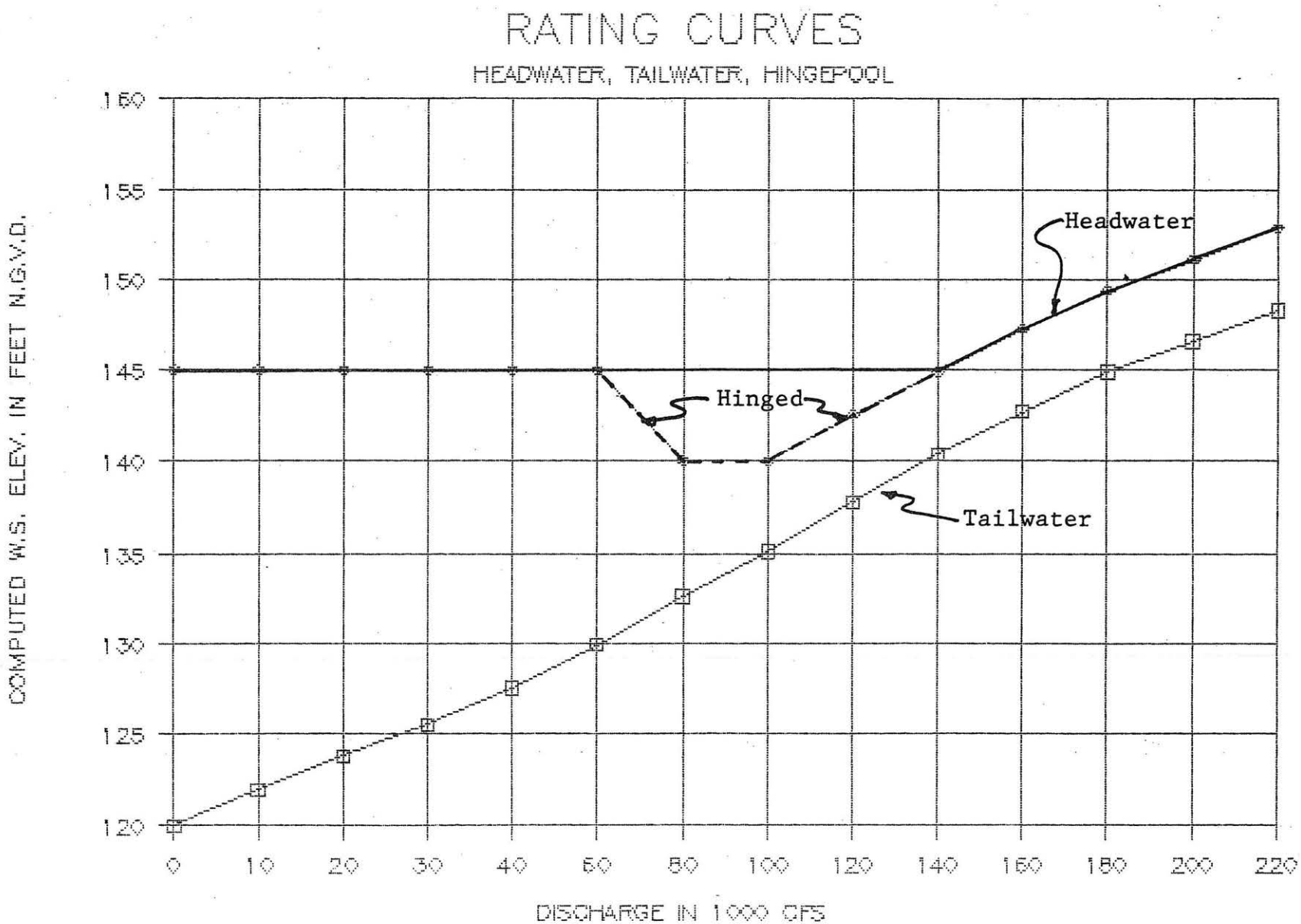
RATING CURVES
HEADWATER, TAILWATER, HINGEPOOL
COMPUTED W.S. ELEV. IN FEET N.G.V.D.
160
155
150
145
140
135
130
125
120
0
10
20
30
40
60
80
100
120
140
160
180
200
220
DISCHARGE IN 1000 CFS
Headwater
Hinged
Tailwater

Figure 5

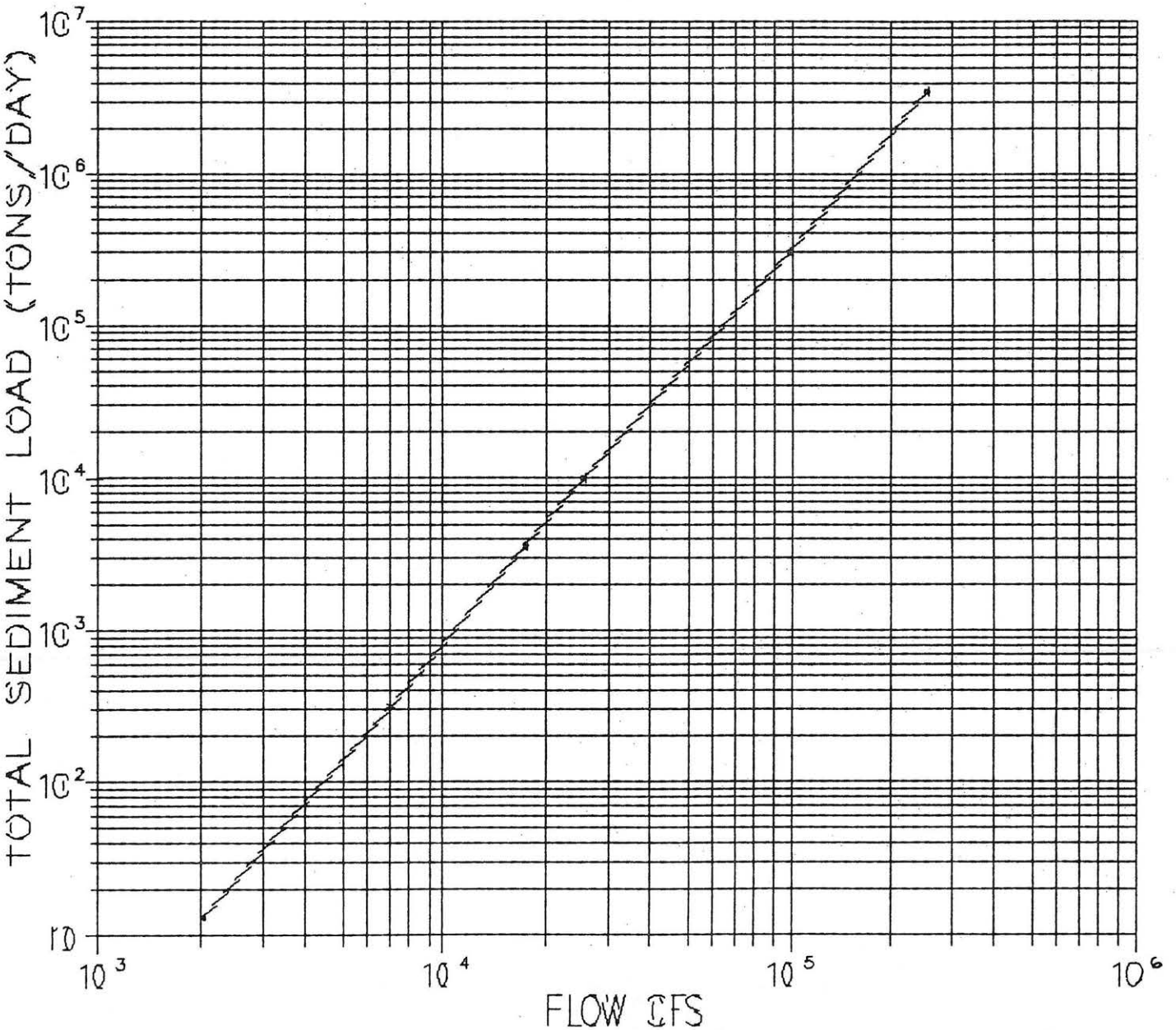
TOTAL SEDIMENT LOAD (TONS/DAY)
10^7
10^6
10^5
10^4
10^3
10^2
10
10^3
10^4
10^5
10^6
FLOW CFS

Figure 6

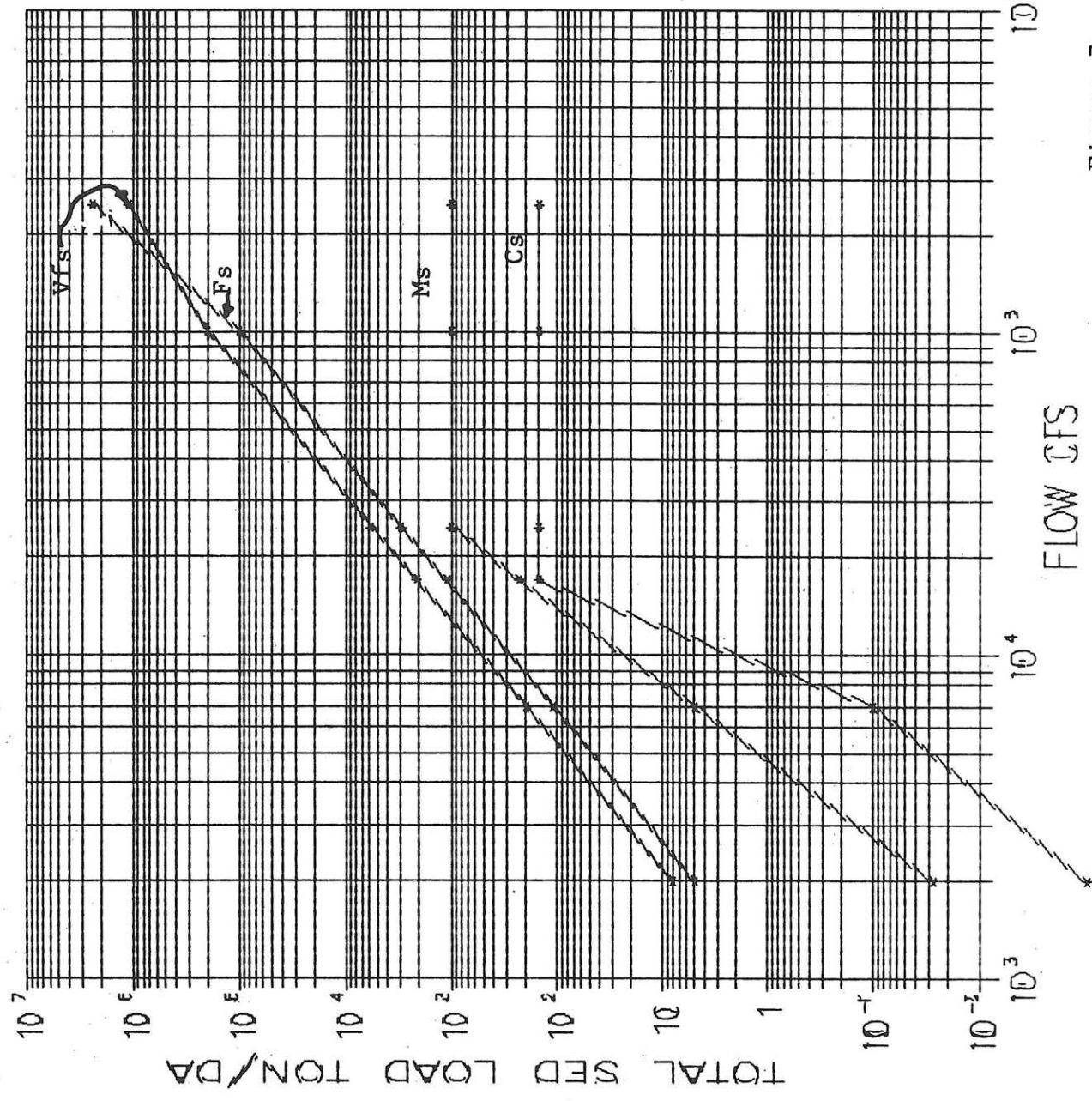

Figure 7

WATER SURFACES & THALWEGS
Toffaleti's

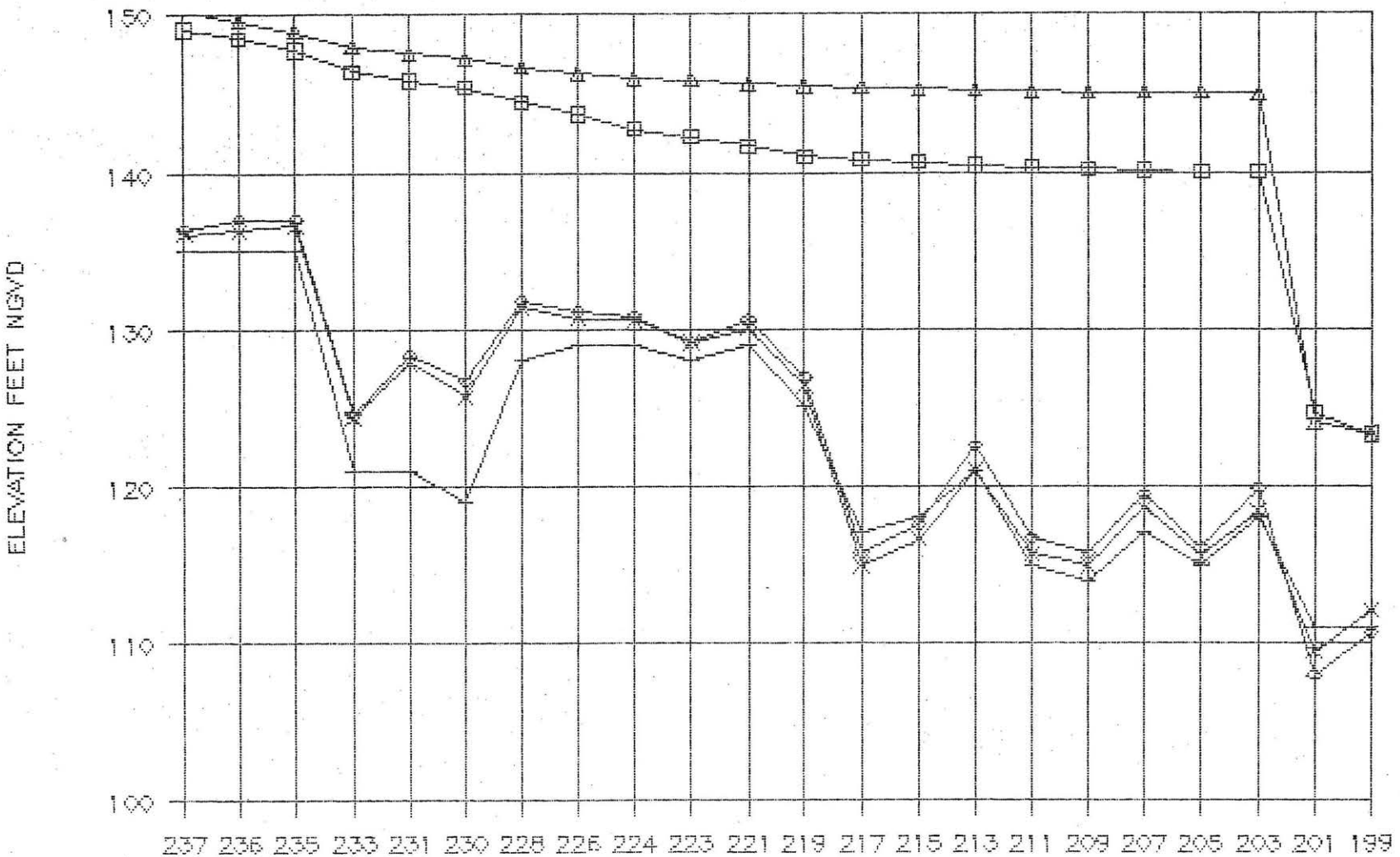

+original thalweg
◊No hinge thalweg
x Hinge thalweg

▲ No hinge WS
□ Hinge WS

Figure 8

THALWEGS (TOFFALETI'S)

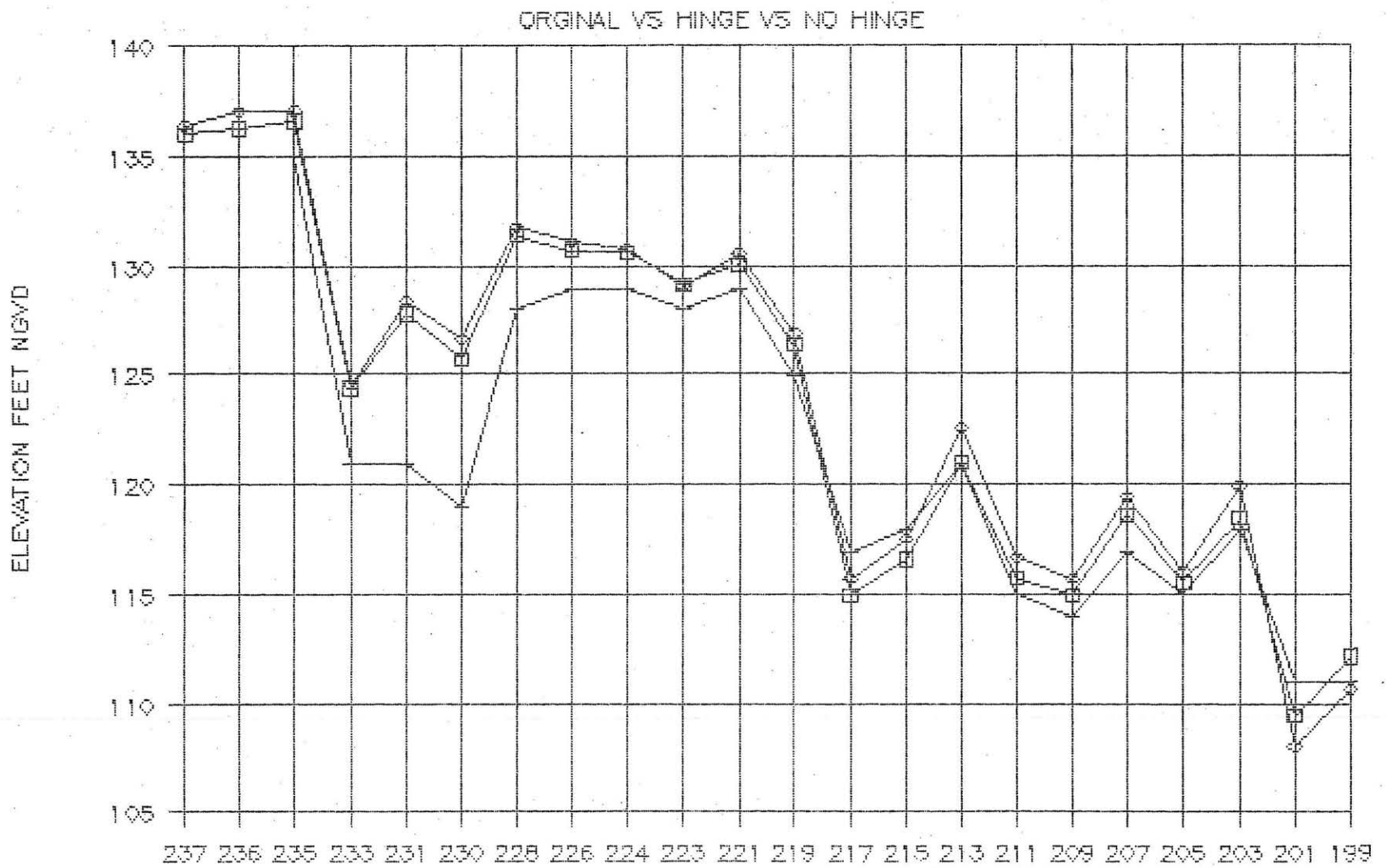

Figure 9

YANGS VS TOFFALETI NO HINGE
Water Surfaces & Thalwegs

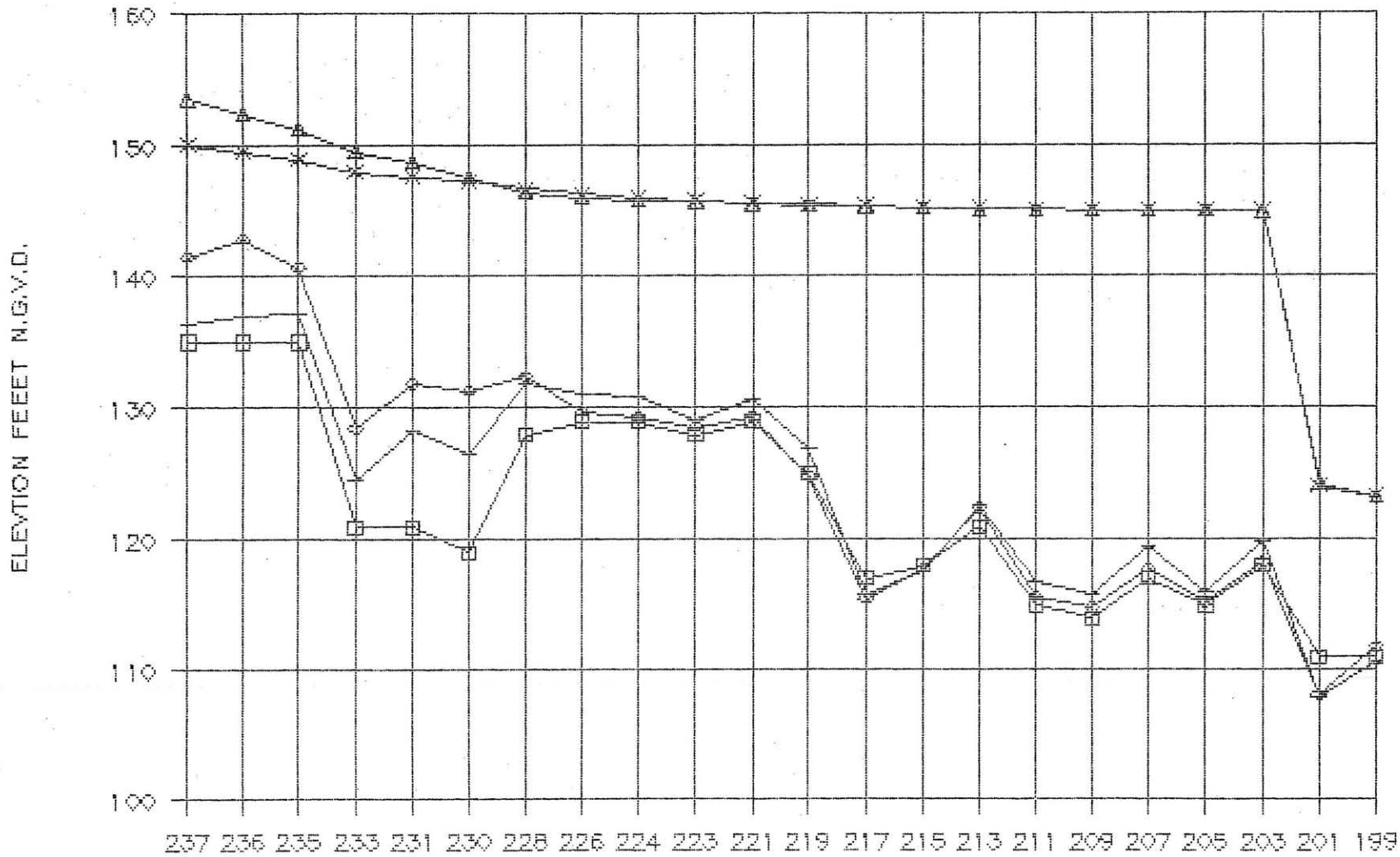

No Hinge WS (Yang)
No Hinge Thalweg (Yang)
Original Thalweg

No Hinge WS (Toff)
No Hinge Thalweg (Toff)

Figure 10

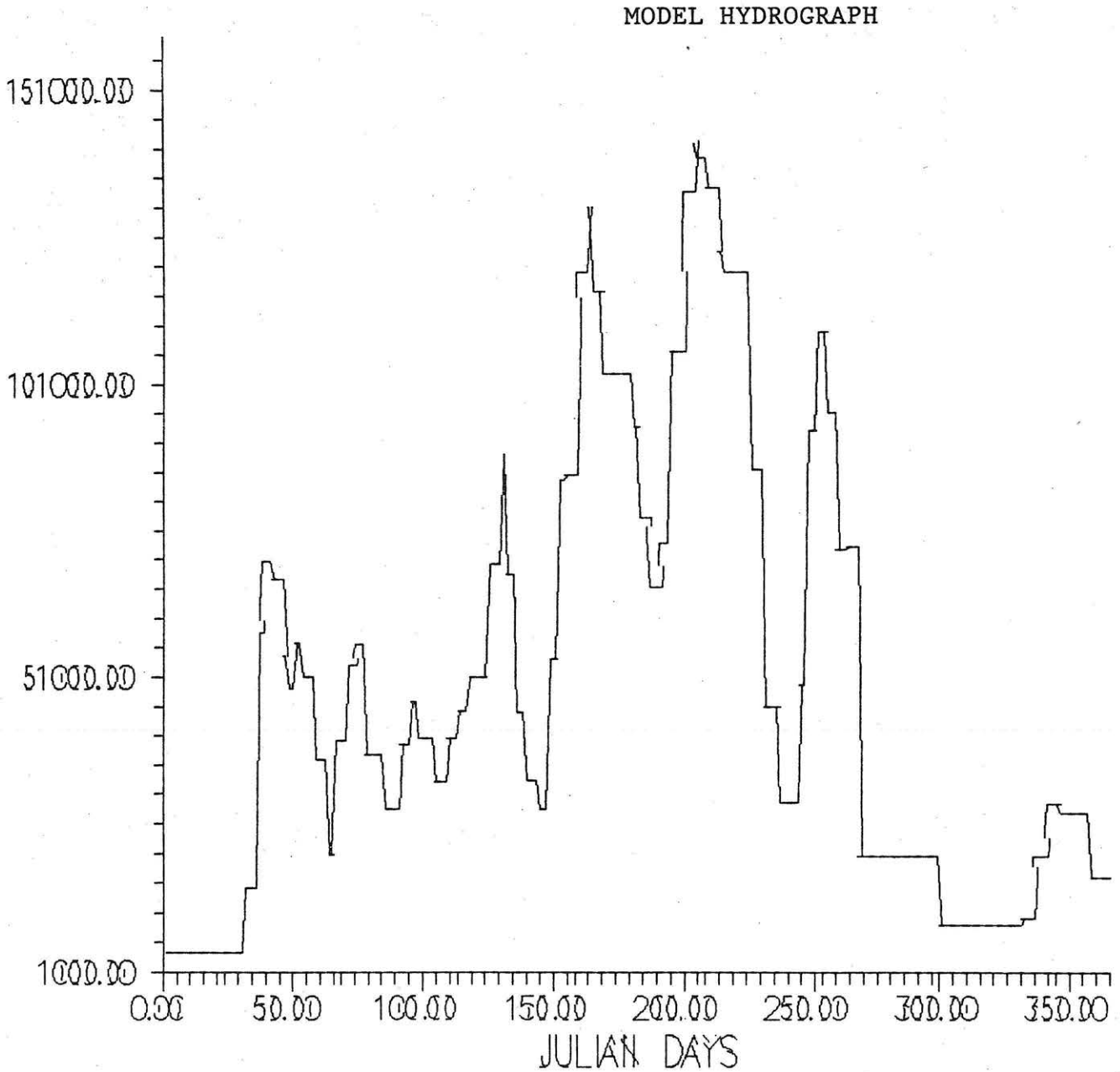
MODEL HYDROGRAPH
151000.00
101000.00
51000.00
1000.00
0.00
50.00
100.00
150.00
200.00
250.00
300.00
350.00
JULIAN DAYS

Figure 11

Bed Degradation Below Dams

By Terry Waddle[1], A.M. ASCE

Abstract: Methods for prediction of stream bed degradation below dams are briefly reviewed as part of the larger problem of predicting channel changes in gravel bed rivers. The difficulties with applying currently available methods to gravel bed rivers are discussed. One state-of-the-art model is summarized as an example of the currently available methods for describing channel aggradation and degradation. An application of one simple method is given; including corrections to the original paper.

INTRODUCTION

The degree of degradation that occurs below a dam is a major concern of any dam project sponsor. Scour by clear, sediment-free water can result in channel changes that may persist for large distances downstream and cause such potential havoc as undermined bridge piers, failed retaining walls or greatly increased maintenance expenses for irrigation and other water diversion activities. The basic process in determining degradation is to combine the continuity equation for sediment with a measure of the erosive capability of the stream such as Shields parameter to determine if there is a net removal of material from the bed. To do so requires defining a critical velocity necessary to produce motion of the bed material. Various means are employed in the models described below to determine either the critical velocity or critical slope, the details of which are contained in the original references.

The need to predict the amount of degradation is clear; however, the methods to do so are still embryonic. To develop a broad understanding of the ability of current methodologies describing fluvial processes in gravel bed streams, particularly the process of degradation below a dam the first section of this paper summarizes the basic contents of recently published methodologies. The second section describes application of a step calculation model to determining the amount of degradation that may occur in a reach of the Salmon River, New York where a braided section of stream is exhibiting characteristics of degradation in a pattern that somewhat resembles a meander cut off. The discussion includes corrections and clarifications for the method (Komura and Simons, 1967) and its summary given in Simons and Senturk (1974).

SUMMARY OF RECENTLY PUBLISHED METHODS AND RESULTS

The problem of degradation below a dam is part of the larger problem of predicting changes in river channels due to various flow events. Since the Salmon River, used as an example in the second portion of this paper, is a gravel and cobble bed stream this summary deals both with methods for characterizing transport phenomena in gravel bed streams and methods for

---

[1]Grad. Student, Dept. of Civil Engineering, Colorado State Univ., Ft. Collins, CO 80523

predicting channel change in beds of finer material. To cover this material, this section progresses from description of sediment movement to dynamic models of channel change.

In an excellent and broadly scoped review of methods of addressing the problem of bedload transport in gravel bed rivers, Carson and Griffiths (1987) discuss the effectiveness of such well known methods as those of Meyer-Peter & Muller, Einstein-Brown, Bagnold and Yalin. They show the results of studies which applied several methods to predicting bed load transport in flumes and in rivers. Unfortunately, even their extensive field data do not permit firm conclusions to be drawn about several methods. However, one conclusion they draw is clear, that is the Bagnold formula consistently under predicts gravel loads in braided channels.

Hey and Thorne (1986) give some regime type equations for mobile gravel-bed rivers that are based on data from 62 rivers in England. Through categorization and regression analysis, they derived equations for width, depth and slope of gravel-bed streams as a function of dominant discharge, sediment size distribution and vegetation influences on the channel. The difficulty in finding a common definition for dominant discharge and the use of regression analysis may limit their conclusions (and the equations derived) to rivers with similar characteristics to those measured.

Komura (1986) describes an empirical approach where aerial photography and basic water and sediment discharge relationships are combined to describe the bed profile of a stream during a high flow event. This approach appears promising from a practical standpoint since the detailed measurements needed for dynamic modeling are often not available for particular rivers of interest.

Beyond methods for describing the channel form and transport rates of bed material lies development of physical process models designed to account for the net change in channel formation as a result of the interaction of water and sediment under a variety of conditions. In 1982 Li and Simons provided a general conceptual guide to development of physical process models of channel change. They classify models into groups based on the quantity of water and sediment being routed, the predominant physical water routing mechanism, and calculation techniques. This classification scheme sets the scene for the next category of models covered here, dynamic models of channel response.

Richardson et al. (1987) give a summary of short term and long term sediment routing models that can predict net aggradation and degradation of a stream reach. These models include an extension to HEC-2 developed by Simons, Li and Associates, an uncoupled unsteady water and sediment routine model developed by Chen and Simons at CSU, FLUVIAL-11 developed by Chang and Hill (discussed below), KUWASER developed by Brown, Simons and Li, HEC-6 developed by the U.S. Army Corps of Engineers, CHAR II developed by a French consulting form and IALLUVIAL developed by Karim and Kennedy. Extensive discussion of these models will not be given here. Interested readers are referred to the respective papers.

Lu and Shen (1986) provided a comparison of several degradation models including some of those referenced above. The models they evaluated were all one dimensional models based on some form of solution of the gradually varied flow equations to obtain a water surface profile (step-backwater or finite difference methods) and modification of the bed elevation based on the sediment continuity equation. The solution methods reviewed include: the diffusion analogy, which provides an analytical solution and finite dif-

ference and finite element methods. Lu and Shen compared the predictions of these model classes with the results of a laboratory experiment by Suryanarayana (1967). They found that all methods over predicted degradation and required correction factors to bring the model results in line with the experiment. Lu and Shen were able to determine approximate boundaries on the corrections used but were not able to determine analytical means of establishing the correction without comparison with measurements.

Chang (1982, 1984) has developed models (FLUVIAL-11, FLUVIAL-14) based on minimizing total stream power applied to a cross section. These models are unique in that they address both lateral as well as longitudinal channel changes. Chang's models have five major components: (1) water routing; (2) sediment routing; (3) changes in channel width; (4) changes in channel-bed profile; and (5) lateral migration of the channel. In 1984, Chang demonstrated a very good fit of FLUVIAL-11 predictions and actual channel changes in the San Dieguito River during two floods in March, 1978 and February, 1980. It should be noted, however, that a discussion of his paper by Beatty (1984) points out that the model has only been applied to a sand bed channel with a narrow range of sediment sizes. The discussion goes on to suggest that the model be tested in streams with a variety of rock and soil conditions and hydraulic gradients to determine its generality.

Conclusions: Recently Published Methods and Results - The techniques and models mentioned above range from definition of stream regimes to complex computer programs. The greatest success in describing degradation seems to be Chang's work where both longitudinal and lateral channel profiles, reflecting aggradation and degradation are predicted. His model has been successful in a sand bed channel, but there is no report of a similar application in a gravel bed stream.

When gravel bed rivers are considered, several problems arise that are related to armoring and the conditions needed to initiate motion. These situations are not adequately handled by the available methods. The New Zealand studies indicate that the well known methods proposed by Einstein-Brown, Meyer-Peter and Muller, and Bagnold are either dependent on estimation of certain difficult to measure parameters or simply do not do well in gravel bed streams. Richardson et al. point out that there is yet no good computer model of the armoring process. Such a lack of a well established analytical technique for gravel bed rivers leaves the engineer with the need to apply very astute judgement when working in this area. The cost of hiring a qualified analyst who has the needed depth of experience is justified by the lack of established analytical methods to predict degradation.

APPLICATION OF A SIMPLE METHOD TO A CASE STUDY

Komura and Simons (1967) developed a step-type calculation of degradation below dams similar to the standard-step method for backwater calculations. The method is based on the observation that clear water releases from a dam tend to remove smaller material from the bed alluvium resulting in a sorting by particle size. It is common for the median grain size, d_{50}, after closure of a dam to be equal to the largest fractions, d_{84} to d_{95}, that were present in the stream bed before closure. Komura and Simons used this information to determine the amount of degradation as an exponential function based on physical parameters and certain corrections for non-uniform particle size.

Due to errors in their original paper and in the summary in Simons and Senturk, portions of their derivation are reproduced and the numerical example given in the paper is re-worked here prior to the application.

From the continuity equation:

$$\frac{\delta Q}{\delta x} + \frac{\delta y}{\delta t} = 0 \quad \text{.....(1)}$$

if the rate of change in the vertical distance from a datum to the bed is Z, its variation with time is dZ/dt (= $\delta y/\delta t$) which gives the rate of change of depth. Taking q_s as the bed load transport per unit width, the sediment transported over the entire width B of the stream is $q_s B$ which varies along the stream as $\delta(q_s B)/\delta x$. Applying this quantity over a unit time produces a volume and the vertical dimension of this volume is $1/(B(1-.))\delta(q_s B)/\delta x$, where . is the porosity of the bed material. Substituting $\delta y/\delta t$ and $\delta Q/\delta x$ into eq. (1) gives:

$$\frac{\delta Z}{\delta t} + \frac{1}{B(1-\lambda)} \frac{\delta(q_s B)}{\delta x} = 0 \quad \text{.....(2)}$$

where: t = time, . = porosity of the bed, q_s = the rate of sediment transport in volume of material per unit time and unit width. Komura and Simons incorporated the equation of motion proposed by Kalinske and Brown (1950) and added the critical friction velocity yielding:

$$q_s = \beta\, d_s^{(1-p)}\, U_\star\, (U_\star^2 - U_{\star c}^2)^p \quad \text{.....(3)}$$

$$\text{in which: } \beta = \frac{a_s}{((\sigma/\rho - 1)\, g)^p} \quad \text{.....(3a)}$$

where: $U_\star$ = friction velocity; d_s = mean bed material diameter; μ and σ are density of water and sediment; g = gravitational acceleration; a_s = a constant; p = a dimensionless exponent. When $(\sigma/\rho) = 2.65$, $a_s = 10$, $p = 2$, and $g = 32.2$ ft/sec^2, β becomes 0.003543 (ft/sec^2)$^{-2}$.

Friction velocity can be expressed as:

$$U_\star = \frac{g^{1/2}\, Q\, n}{1.486\, B\, y^{7/6}} \quad \text{.....(4)}$$

where: n = Manning's coefficient, Q = water discharge, y = depth of flow. Differentiating this equation with respect to x yields:

$$\frac{\delta U_\star}{\delta x} = \frac{U_\star}{n} \left(\frac{\delta n}{\delta x} - \frac{7n}{6y}\frac{\delta y}{\delta x} - \frac{n}{B}\frac{\delta B}{\delta x}\right) \quad \text{.....(5)}$$

Considering the effects of armoring, Komura expressed the friction velocity as:

$$U_\star = \sqrt{a_c'\, (\sigma/\rho - 1)\, g\, d_s} \quad \text{.....(6)}$$

where: $a_c' = a_c\, C_a = a_c\, \varepsilon\, Sd^r$, a_c = a function of the critical shear velocity Reynolds number, $U_{\star c} d_s/v$, v = kinematic viscosity of water, C_a = an armoring

coefficient, ε = a constant, r = a dimensionless exponent, and Sd = standard deviation of the particle size distribution of river-bed size fractions. Sd is defined as:

$$Sd = \sqrt{\frac{d_{84}}{d_{16}}} \quad \text{.....(7)}$$

The value of a_c is obtained from Figure 1. Figure 1. has been re-derived for this example by selecting particle size - a_c pairs from the original figure given by Komura and Simons and calculating the critical shear velocity Reynolds number. A slight variation from their original figure resulted that may be attributable to the computational devices available at the time of the original calculations.

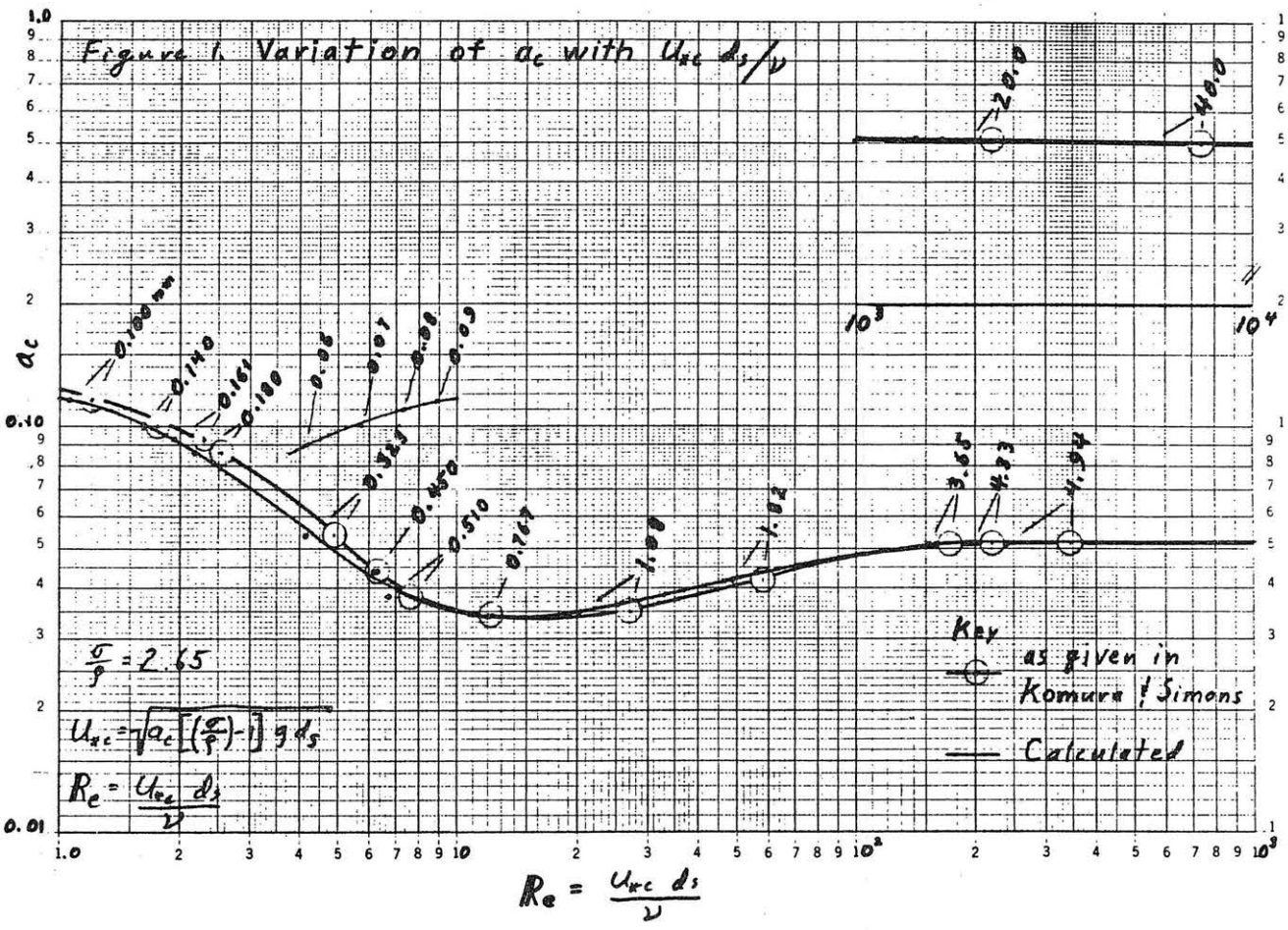

Figure 1. Variation of a_c with Critical Shear Reynolds Number

Komura and Simons found values of r ranging from 0.7 to 1.75 experimentally. They use r = 1 in their paper. They also give $\varepsilon = 1$ because $a_c' = a_c$ when Sd = 1 and note that Egiazaroff (1965) proposed an alternative definition of a_c':

$$a_c' = \frac{0.1}{(\log_{10} 19\ (d_{50}/d_g))^2} \quad \text{.....(8)}$$

where: d_g = the grain size which determines the roughness of the bed.
Equation 2 can be re-written as:

$$\frac{\delta Z}{\delta t} = - \frac{1}{(1-\lambda)} \frac{\delta q_s}{\delta x} - \frac{q_s}{B(1-\lambda)} \frac{\delta B}{\delta x} \quad \ldots\ldots (9)$$

Substituting eq. 3, 6, $\delta U_{*c}/\delta x$ from eq. 7, and $\delta n/\delta x$ from Chow (1959) into eq. 9, rearranging, setting p = 2, and simplifying using approximations supplied by Komura and Simons yields:

$$\frac{\delta Z}{\delta t} = \frac{2\,\beta}{(1-\lambda) d_s} U_*^3 \,(U_*^2 - U_{*c}^2)\, \left(\frac{1}{6 d_s} \frac{\delta d_s}{\delta x} + \frac{7}{3\,y} \frac{\delta y}{\delta x} + \frac{2}{B} \frac{\delta B}{\delta x}\right) \quad \ldots\ldots (10)$$

The final equilibrium state after degradation has taken place would occur when $\delta Z/\delta t = 0$. Under that condition, eq. 10 reduces to:

$$U_{*f}^2 = U_{*cf}^2 = C_s\, g\, d_{sf} \quad \ldots\ldots (11)$$

and

$$\frac{\delta y_f}{\delta x} = - \frac{3}{7} \left(\frac{y_f}{6\, d_{sf}} \frac{\delta d_{sf}}{\delta x} + \frac{2\, y_f}{B} \frac{\delta B}{\delta x}\right) \quad \ldots\ldots (12)$$

in which $C_s = a_c'\,(\sigma/\rho - 1)$ and the subscript f indicates final equilibrium state.

When the bed of a rectangular channel has attained equilibrium, Komura derives the bed slope as:

$$S_{fb} = C_s \left(\frac{d_{sf}}{y_f} \right) - \frac{1}{14} \left(1- \frac{y_c^3}{y_f^3}\right) \left(\frac{y_f}{d_{sf}}\right) \frac{\delta d_{sf}}{\delta x}$$

$$- \frac{1}{7} \left(\frac{y_f}{B} \right) \left(6 + \frac{y_c^3}{y_f^3}\right) \frac{\delta B}{\delta x} \quad \ldots\ldots (13)$$

where $y_c^3 = \alpha\, Q^2/g\, B^2$, $\alpha = 1$, and y_c = the critical depth of flow. Final bed slope is defined by $S_{fb} = -(\delta Z_f/\delta x)$. Thus taking the x' axis in the downstream direction, the final river bed elevation can be expressed as:

$$Z_f = Z_o + \int_o^{x'} \left[C_s \left(\frac{d_{sf}}{y_f}\right) + \frac{1}{14} \left(1- \frac{y_c^3}{y_f^3}\right) \left(\frac{y_f}{d_{sf}}\right) \frac{\delta d_{sf}}{\delta x'}\right.$$

$$\left. + \frac{1}{7} \left(\frac{y_f}{B}\right) \left(6 + \frac{y_c^3}{y_f^3}\right) \frac{\delta B}{\delta x'}\right] dx' \quad \ldots\ldots (14)$$

For a constant width stream, $\delta B/\delta x' = 0$. Then the sediment size variation along the river can be expressed as $d_{sf} = d_{sfo} = e^{cx'}$ and eq. 12 becomes:

$$\frac{\delta y_f}{\delta x'} = - \frac{c}{14}\, y_f \quad \ldots\ldots (15)$$

Because $y_f = y_{fo}$ at $x' = 0$, integration of eq. 15 yields:

$$y_f = y_{fo}\, e^{-\frac{c}{14} x'} \quad \text{.....(16)}$$

Substituting eq. 16 into eq. 13 yields an expression for the final equilibrium profile for a constant width:

$$Z_f = Z_o + \frac{14}{15}\left(\frac{C_s}{c}\right)\left(\frac{d_{sfo}}{y_{fo}}\right)\left(e^{(15c/14)x'} - 1\right)$$

$$+ y_{fo}\left(1 - e^{(-c/14)x'}\right) - \frac{y_{fo}}{2}\left(\frac{y_c}{y_{fo}}\right)^3 \left(e^{(c/7)x'} - 1\right) \quad \text{.....(17)}$$

Numerical Example - Komura and Simons give a numerical example that has several flaws. Unfortunately, Simons and Senturk quote the example without correcting errors or properly identifying how certain values were derived. Further, Simons and Senturk reference equations that are omitted from the text. This discussion attempts to fill in those gaps.

The example concerns degradation below the Milburn Diversion Dam on the Middle Loup River in Nebraska. Values of a_c are obtained from Figure 1 for the mean particle size. The variance (not standard deviation as stated in the paper) is used to scale a_c to a_c' for consideration of sorting and armoring due to effects of release of clear water. Table 1 shows the values obtained by working the example using the instructions given by Komura and Simons. A composite value of a_c' of 0.344 is obtained and brought forward to the next step.

Table 2 illustrates the step method considering two cases. Most of the table is devoted to deriving the discretized form of the terms in equation 17. Though not developed here, the discretized form of the equation allows variable width among the reaches and requires a backwater model be applied as part of the calculation. The columns have the following meanings and computations: column 1, reach identifier; column 2, distance from reach i to the downstream reference point (x'); column 3, individual reach length; column 4, reach width; column 5, change in reach width; column 6, final mean particle size, $D_{sf} = D_{sfo} \exp(c\, x')$; column 7, change in mean particle size between reaches; column 8, final depth of flow, $y_f = y_{fo} \exp((-c/14)\ x')$ for constant width and y_f = value from backwater model for variable width case; column 9, cube of mean critical depth in reach, $(y_c^3)_m = \alpha\ Q^2/g\ B^2$, $\alpha = 1$; column 10, ratio of critical depth cube to final depth cube, $(y_c^3/y_f^3)_m$; column 11, average depth-width ratio, $(y_f/B)_m$; column 12, average depth-particle size ratio, $(y_f/D_{sf})_m$; column 13, change in bed elevation,

$$\Delta Z_f = C_s\left(\frac{d_{sf}}{y_f}\right)_m \Delta x' + \frac{1}{14}\left[1 - \left(\frac{y_c^3}{y_f^3}\right)\right]\left(\frac{y_f}{d_{sf}}\right)\frac{\delta d_{sf}}{\delta x'}$$

$$+ \frac{1}{7}\left(\frac{y_f}{B}\right)\left[6 + \left(\frac{y_c^3}{y_f^3}\right)\right]\Delta B \quad \text{.....(18);}$$

column 14, bed elevation from numerically integrating changes in bed elevation; and column 15, bed elevation from eq. 17 with coefficients and exponents as described below. Equation 18 is omitted in Simons and Senturk.

Exponents and Coefficients used in Example - With $r = \varepsilon = 1$ and $a_c' = a_c * Sd$; then from Table 1, Sd = 3.762 and a_c = 0.091 so a_c' = 0.344. $C_s = a_c'\,(\sigma/\rho - 1)$; 0.344 * 1.65 = 0.567. c = 0.00011 ft^{-1}; the value given

Table 1. Sediment Properties of Middle Loop River Bed

Range No.	x' (ft)	d16 (mm)	d50 (mm)	d84 (mm)	d90 (mm)	SIGphi	var SigPhi	ac from plot	ac'
1	17850	0.052	0.115	0.250	0.300	2.193	4.808	0.110	0.529
2	14000	0.150	0.240	0.430	0.520	1.693	2.867	0.070	0.201
3	0	0.036	0.061	0.130	0.170	1.900	3.611	0.094	0.339
--	-----	-----	-----	-----	-----	-----	-----	-----	-----
Averages			0.139			1.929	3.762	0.091	0.344

Table 2. Example Computation by Step Method For Q = 780 cfs

eta	x'	Del x' eta	B	Del B eta	Dsf	Del Dsf eta	(Yf)m	(Y^3c)m	(Y^3c/ Y^3f)m	(Yf/B)m	(Yf/ Dsf)m	Del Zf eta	Zf eta Var Width eqn. 28	Zf eta Con Width eqn. 30
	ft	ft	ft	ft	ft	ft	ft	ft^3				ft	ft	ft
(1)	(2)	(3)	(4)	(5)	(6)	(7)	(8)	(9)	(10)	(11)	(12)	(13)	(14)	
7	18600	750	300	0	0.00292	0.000211	1.12	0.210	0.149	0.00374	384	1.11	13.68	9.49
6	17850	1750	300	-50	0.00271	0.000435	1.13	0.210	0.147	0.00376	416	2.23	12.57	8.60
5	16100	2100	350	-50	0.00228	0.000431	1.14	0.154	0.104	0.00326	501	2.25	10.34	6.79
4	14000	2900	400	50	0.00184	0.000464	1.16	0.118	0.076	0.00290	628	2.76	8.09	5.06
3	11100	2500	350	50	0.00138	0.000305	1.18	0.154	0.093	0.00338	857	1.82	5.33	3.26
2	8600	2500	300	-50	0.00108	0.000237	1.20	0.210	0.120	0.00401	1120	1.11	3.51	2.13
1	6100	6100	350	0	0.00084	0.000382	1.23	0.154	0.084	0.00350	1464	2.40	2.40	1.29
0	0.00001	0	350	0	0.00045	0	1.28	0.154	0.074	0.00366	2814	0.00	0.00	0.00

Where the following constant values were used in the calculations: c = 0.0001 =Dsf/(Dsfx'), Dsfo = 0.139 mm = 0.000454 ft., Gams' = 1.65, Cs = ac' Gams', ac' = 0.344, Cs = 0.5669, and g = 32.174 ft/sec^2.

by Komura and Simons. D_{sfo} = mean particle size at downstream control = 0.000454 ft. Note, in their article, Komura and Simons derive D_{sfo} as .139 mm in Table 1 and then erroneously use .130 mm in Table 2. The value .139 mm is used here. y_{fo} = depth at downstream control given = 1.28 ft. y_{co} = critical depth at downstream section (same for constant width case) = .554 ft. B = width = 350 ft. Z_o = reference elevation = 0.

Example Results - Table 2 gives the results of the step calculation. The maximum degradation calculated is 13.68 ft. which compares with 12.26 ft. given in Komura and Simons original paper. The differences can be attributed to three sources. First, they did not properly obtain a_c' so the adjustment for armoring was low by about 40% (0.25 in the paper as opposed to 0.344 obtained here). Second, they appear to have used a backwater model to get the depth of flow in each reach instead of the exponential function given. This resulted in less depth in most sections. Third, their example has variable width which also influences the depth of flow and depth-width ratio. Considering these differences, the method is surprisingly robust for the given data set since the calculated degradation depths only differed by about 1.4 ft.

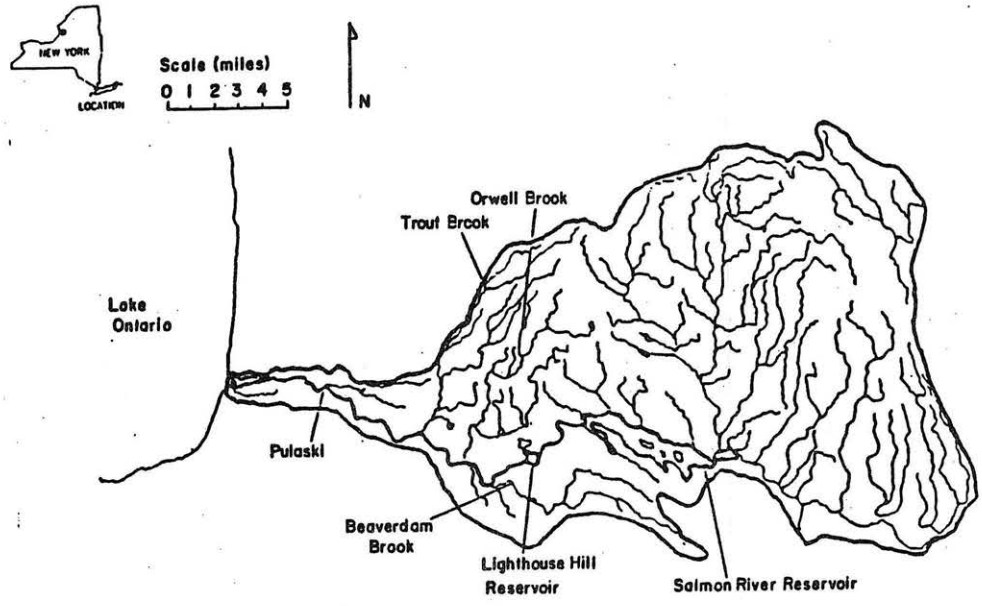

Figure 2. Salmon River Location Map

APPLICATION TO THE SALMON RIVER

Basin Description - The Salmon River (Figure 2) drains 692 sq. km (267 sq. mi) of the southwest portion of the Tug Hill Plateau. It flows through the Niagara Mohawk Salmon River Project facilities near Bennets Bridge and Altmar, in Oswego County, N.Y., and drains into Lake Ontario at Selkirk. The Salmon River Project consists of two reservoirs and powerplants. The upstream reservoir, Salmon River Reservoir, has a storage capacity of about 82 million cubic meters (66,600 acre ft). It is about 10.2 km (6.4 mi) long

and 1.2 km (0.8 mi) wide. It has an area of about 13.5 sq. km (5.2 sq. mi) which gives it a relatively high area to volume ratio. Its spillway has an elevation of 286 m (937 ft) above sea level giving a drop of about 87 m (286 ft) to the lower reservoir.

Lighthouse Hill Reservoir receives the discharge from the upper reservoir through the Bennets Bridge Power plant and through the relic Salmon River channel in times of flood. The lower reservoir has a surface area of 0.67 sq. km (0.26 sq. mi) and a volume of 3.9 million cubic meters (3100 acre ft). Due to its relatively small size this reservoir has little effect on discharge during flood events or on water temperature during most of the year. The elevation profile is given in Figure 3.

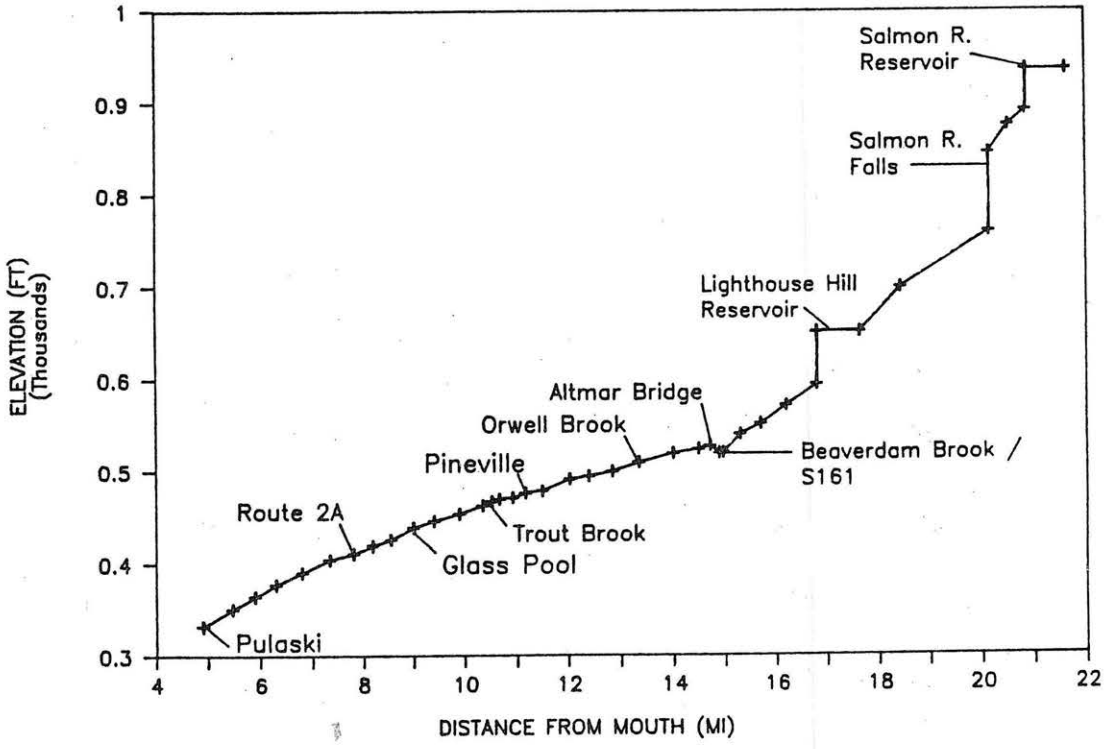

Figure 3. Salmon River Elevation Profile

The Lighthouse Hill power plant has two turbine and generator units. During the 1986 study period the operation of the lower reservoir consisted of periods of one or two unit generation at Lighthouse Hill separated by idle periods. When the plant is not generating, leakage of about 0.566 cms (cubic meters per second), that is 20 cfs (cubic feet per second) supplies the stream channel with a minimum discharge as shown in the figure. A low release of approximately 10 cms (350 cfs) is occasionally made to reduce the water temperature at the Salmon River Hatchery located 3.6 km (2.3 mi) downstream. This release is commonly referred to as a one-half unit release as it provides about one-half the discharge produced by one turbine operating in its most efficient range. The degradation component of this study is based on a two unit release of 1500 cfs.

The study reach is located above Altmar about 4 km (2.9 mi) downstream from lighthouse hill reservoir. The greater part of the flow proceeds southwest around the island shown in Figure 4 and merges with the discharge from Beaverdam Brook. The northern side channel did not regularly carry

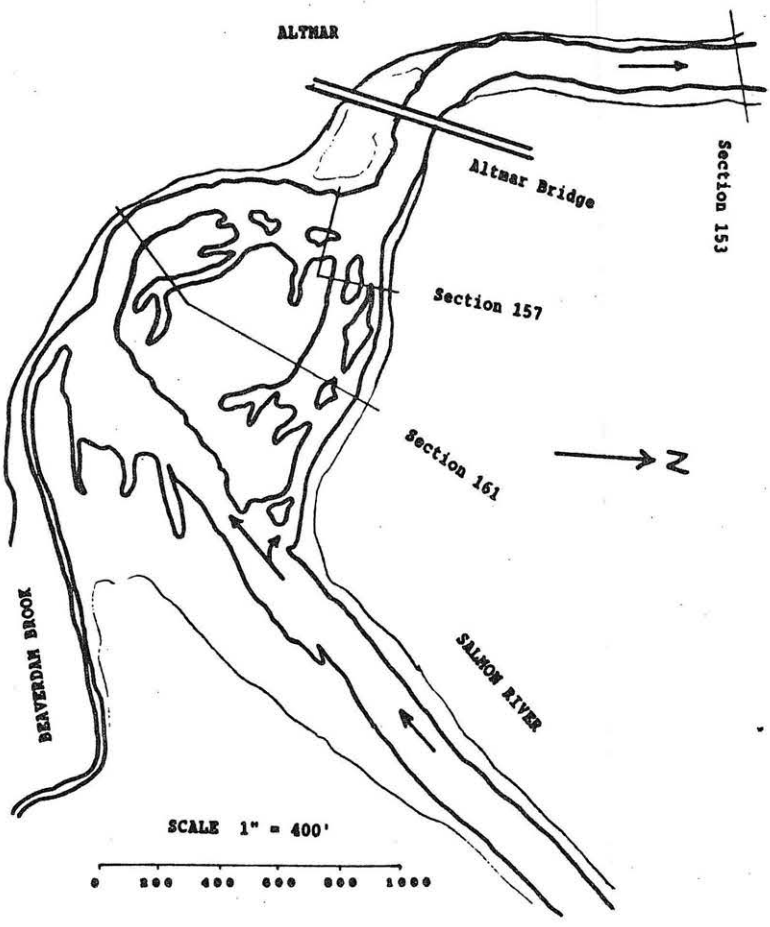

Figure 4. Study Site Map

water until a flood in December of 1984 altered the channel entrance such that the higher flows of a two unit operation can now pass through that channel. Three transects have been established in the area as shown on the map. Section 153 is assumed to act as a control, though the bridge may over ride it at high flows.

Available Sediment Data - Sediment data for this river was available in the form of a surface and subsurface sieve sample taken at Altmar and surface samples taken near Altmar. The second surface sample was taken near section 153 using a tape measurement method. The short, median and large axis dimensions of the particles found at each of 23 one foot intervals were recorded. The sieve size equivalent of these particles was obtained by estimating if the two smaller dimensions of each particle would fit through the sieve grid. This estimating method assumed rectangular particles. The weight ratio of the surface and subsurface material was obtained by assuming a porosity of 0.3 for the surface material and 0.1 for the subsurface

material. These ratios were varied to test the sensitivity of this assumption. It was found to be relatively insensitive. This data is summarized in Table 3. The d_{16} and d_{84} values used in finding the variance in particle size (Sd) were obtained from Figure 5.

Table 3. Development of Combined Sediment Size Distribution

Sieve Size	Tape Fraction In Sieve Size By Volume	Subsurface Sieve Fraction	Subsurface Fraction Scaled	Weighted Sum	Normalized Frequency	Cumulative Frequency	Plot Position	Size Frac (in)
12"	0							
9"	0.042	—	0.000	0.042	0.018	1.000	0.935	9.000
6"	0.333	—	0.000	0.333	0.146	0.982	0.918	6.000
3"	0.458	0.392	0.504	0.962	0.421	0.836	0.781	3.000
3/2"	0.167	0.161	0.207	0.374	0.164	0.414	0.387	1.500
3/4"		0.206	0.265	0.265	0.116	0.251	0.234	0.750
3/8"		0.093	0.120	0.120	0.052	0.135	0.126	0.375
3/16"		0.058	0.075	0.075	0.033	0.082	0.077	0.188
#8		0.030	0.039	0.039	0.017	0.050	0.046	0.094
#16		0.011	0.014	0.014	0.006	0.033	0.031	4.69E-02
#30		0.009	0.012	0.012	0.005	0.026	0.025	2.34E-02
#50		0.023	0.030	0.030	0.013	0.021	0.020	1.17E-02
#100		0.011	0.014	0.014	0.006	0.008	0.008	5.86E-03
#200		0.003	0.004	0.004	0.002	0.002	0.002	2.93E-03
#200+		0.001	0.001	0.001	0.001	0.001	0.001	1.46E-03
					2.283	1.000		

Note: Sieve Size equivalent of Tape measurement method surface material obtained by estimating if two smaller dimensions of each particle would fit through sieve grid. The estimating method assumed rectangular particles. This approach was used to better differentiate among particles that passed a 12 in. sieve and were held by the 6 in. sieve, allowing D84 to be more clearly identified.

The ratio of weight for the surface and subsurface material was obtained by assuming a porosity of 0.3 for the surface and 0.1 for the subsurface material.

Tables 4 and 5 show the results of the initial calculation of degradation. Since only one sediment sample was available, it was assumed to represent all sites. The value of a_c and the variance Sd were relatively large. When multiplied, they produced a value of a_c' of 3.677. The resulting degradation depth predicted by the method was 517 ft. If this were true, the Salmon River would have sufficient erosive power to remove the entire state of New York. A possible cause of this over-prediction of degradation was the a_c' value. When Egiazaroff's value was calculated and substituted in the method (Table 6) much more likely values of degradation from 13.76 to 14.86 ft were obtained. Since the main channel at section 161 has a pool that has scoured to a depth of about 12 ft relative to the current side channel thalweg it is possible that these values are within reason.

Table 4. Sediment Properties of Salmon River Bed

d16 (mm)	d50 (mm)	d84 (mm)	d90 (mm)	SIGphi	var SigPhi	ac from plot	ac'
12.700	46.400	93.400	130.000	2.712	7.354	0.500	3.677

Table 5. Salmon River Computation by Step Method For Q = 780 cfs

eta	x'	Del x' eta	B	Del B eta	Dsf	Del Dsf eta	(Yf)m	(Y^3c)m	(Y^3c/ Y^3f)m	(Yf/B)m	(Yf/ Dsf)m	Del Zf eta	Zf eta Var Width eqn. 28	Zf eta Con Width eqn. 30
	ft	ft	ft	ft	ft	ft	ft	ft^3				ft	ft	ft
(1)	(2)	(3)	(4)	(5)	(6)	(7)	(8)	(9)	(10)	(11)	(12)	(13)	(14)	
2	2020.000	320	200	0	0.18631	0.005867	4.29	0.473	0.006	0.02144	23	84.37	517.49	478.91
1	1700.000	1700	200	0	0.18044	0.028208	4.30	0.473	0.006	0.02149	24	433.12	433.12	395.97
0	0.00001	0	200	0	0.15223	0	4.35	0.473	0.006	0.02175	29	0.00	0.00	0.00

c = 0.0001 = Del Dsf/(Dsf*Del x')
Dsfo 46.400 mm
Dsfo 0.152229 ft
Gams'Gams/Gam - 1 = 1.65
Cs = ac' Gams'
Yfo = 4.35 ft.
ac' = 3.677
Egiazaroff ac'0.1052
Cs = 6.0673
g = 32.174 ft/sec^2

Computation for Salmon River using Komura and Simons method as given in their original paper. Note excessive degradation.

Table 6. Salmon River Computation by Step Method For Q = 780 cfs

eta	x'	Del x' eta	B	Del B eta	Dsf	Del Dsf eta	(Yf)m	(Y^3c)m	(Y^3c/ Y^3f)m	(Yf/B)m	(Yf/ Dsf)m	Del Zf eta	Zf eta Var Width eqn. 28	Zf eta Con Width eqn. 30
	ft	ft	ft	ft	ft	ft	ft	ft^3				ft	ft	ft
(1)	(2)	(3)	(4)	(5)	(6)	(7)	(8)	(9)	(10)	(11)	(12)	(13)	(14)	(15)
2	2020.000	320	200	0	0.18631	0.005867	4.29	0.473	0.006	0.02144	23	2.42	14.86	13.76
1	1700.000	1700	200	0	0.18044	0.028208	4.30	0.473	0.006	0.02149	24	12.44	12.44	11.38
0	0.00001	0	200	0	0.15223	0	4.35	0.473	0.006	0.02175	29	0.00	0.00	0.00

Computation for Salmon River using Komura and Simons method with adjustment. Egiazaroff's value of ac' is used instead of Simons and Komura. All other Constants and coefficients as above.

Conclusions From Case Study - The original Komura and Simons paper had numerous errors. Those problems were worked out and the method predicted approximately the same degradation as the example in the original paper. Their work, however, was in a sand bed channel. There was no reference to extending the model to gravel bed streams; however, their relationship for deriving a_c (Figure 1) extended to a particle size of 40 mm which was very near the mean particle size of 46.4 mm found in the Salmon River. It is not clear that the method was intended to be used over the full range of a_c values given. As is often the situation in gravel bed streams a considerable amount of judgement must be used in applying this model. Applying the model exactly as presented by Komura and Simons resulted in prediction of 517 feet of degradation. Use of Egiazaroff's value of a_c' produced a much more reasonable range of degradation values between 13.76 and 14.86 ft. Since it was necessary to ignore the Komura and Simons adjustment for armoring and fall back to an empirical value for a_c' that was based on much smaller particles, it appears that use of this model does not appear to be warranted in gravel bed streams without exercising cautious judgement in its application and in interpretation of the results.

Appendix I. -- REFERENCES

Beatty, David A., Discussion of "Modeling of River Channel Changes" by Howard H. Chang, Journal of the Hydraulics Division, ASCE, Vol. 110, No. 2, Feb. 1984.

Carson, M. A. and G. A. Griffiths, "Bedload Transport in Gravel Channels", New Zealand Journal of Hydrology, Vol. 26, No. 1, Special Issue, 1987.

Chang, Howard H., "Mathematical Model for Erodible Channels", Journal of the Hydraulics Division, ASCE, Vol. 108, No. Hy5, May, 1982.

Chang, Howard H., "Modeling of River Channel Changes", Journal of the Hydraulics Division, ASCE, Vol. 110, No. 2, Feb., 1984.

Chow, Ven Te, Open Channel Hydraulics, McGraw-Hill Book Co. Inc., New York, 1959, p. 206.

Egiazaroff, I. V., discussion of "European Concepts of Sediment Transportation" by J. L. Bogardi, Journal of the Hydraulics Division, ASCE, Vol. 91, No. HY5, Sept., 1965.

Hey, Richard D. and Colin R. Thorne, "Stable Channels with Mobile Gravel Beds", Journal of the Hydraulics Division, ASCE, Vol. 112, No. 8, Aug., 1986.

Kalinske, A.A. and C.B. Brown, "Equations for Sediment Transport", in Engineering Hydraulics, Hunter Rouse, ed., John Wiley and Sons, 1950, p 797.

Komura, Saburo and Daryl B. Simons, "River-bed Degradation Below Dams", Journal of the Hydraulics Division, ASCE, Vol. 93, No. HY4, July, 1967.

Komura, Saburo, "Method for Computing Bed Profiles During Floods", Journal of the Hydraulics Division, ASCE, Vol. 112, No. 9, Sept., 1986.

Lu, Jau-Yau and Hsieh W. Shen, "Analysis and Comparisons of Degradation Models", Journal of the Hydraulics Division, ASCE, Vol. 112, No. 4, April, 1986.

Preissmann, A., "Propagation des intumenscences dans les Canaux et Rivieres," First Congress of the French Association for Computation, Grenoble, France, Sept., 1961.

Richardson, E.V., D.B. Simons and P.Y. Julien, Highways in the River Environment, U.S. Dept. of Transportation, Federal Highway Administration, Jan. 1987.

Simons, Daryl B. and Fuat Senturk, Sediment Transport Technology, Water Resources Publications, Ft. Collins, CO, 1977, pp. 716-731.

Suryanarayana, B., "Mechanics of Degradation and Aggradation in a Laboratory Flume," Ph. D. dissertation, CSU, Ft. Collins, CO, 1969.

Appendix II. -- Notation

The following symbols are used in this paper:

a_c = a function of the critical shear velocity Reynolds number
a_c' = ac adjusted for armoring effects
B = channel width
C_a = armoring coefficient
C_s = $a_c' (\sigma/\mu - 1)$
d_g = grain size determining bed roughness
d_s = bed grain size
n = Mannings n
p = a dimensionless exponent
Q = discharge of water
q_s = sediment discharge rate per unit width
r = a dimensionless exponent
S_d = standard deviation of bed particle size
t = time
U* = friction velocity
x = longitudinal distance
y = depth of flow
Z = vertical distance from a datum to the bed

λ = porosity of the bed
σ = density of sediment
μ = density of water

subscripts
c = critical condition for initiation of motion
f = final equilibrium state

LOCAL SCOUR AT ABUTMENT

P.Y.Julien & Choi,Gye Woon

ABSTRACT

General research about local scour at abutment through literature review and quantitative comparisons of local scour depth was carried out. The mechanism of local scour at abutment is very complex, but it has been known that the major causes about local scour at abutments are vortex systems: the horseshoe vortex system,the wake vortex system,and the trailing vortex system.

A case in the IOWA Highway Research Board No.8 (7) was picked up for quantitative comparison between suggested formulae. Because most formulae were carried out with different condition,experimental equipments and materials,quantitative comparison of local scour at abutment is not confined within narrow limits. So,verification by field measurement data is needed to verify the conformity of model and prototype.

Also,for application in designing,the study for the relationship between channel width, abutment width and upstream width between abutments should be studied and opening ratio by only channel width is not suitable.

INTRODUCTION

Because successive river reaches are of different erodibility,the depth and slopes intend to be different;greater resistance to erosion will give narrower and deeper cross sections. Scour is occurred in the contracted reach,not in the nonuniform flow on the transitions between the wide and narrow reaches. Among the contracted reach ,scour starts at the head of the contraction and proceeds downstream. There are three types of scour in interrelated phenomena:General scour,Contraction scour and Local scour.

As stream flow velocity increases at a bridge constriction,the sediment transport capacity of the flow increases as well.Larger capacity for transport of sediment can cause scouring of the bed in the vicinity of a bridge,and this phenomena is a typical local scour.

Scour in the local vicinity of an abutment can be particularly severe because of the large concentration of flow there and because of vortex systems that form as water flows around the abutments.

The large flow velocities and vortices that develop at an abutment can erode channel and cause the formation of a scour hole in the bed surrounding an abutment. Fig.1 shows local scour phenomena at abutment. As Fig.1 shows,reduced cross section and unchanged discharge without losses makes the velocity in the section 2-2 faster than that in the cross section 1-1 and local scour is occurred in area "A" because of large velocities and vortices.

Local scour at abutment can be separated into two distinct classes depending on whether or not sediment is supplied to a scour hole: Clear water scour and Live bed scour. Clear water scour occurs when

the flow approaching a scour hole is not to transport bed materials or when sediment moved by the flow is much finer than the material forming the scour hole. Live bed scour occurs when a scour hole is continuously supplied with sediment that is of the same size as the material forming the bed of scour hole.

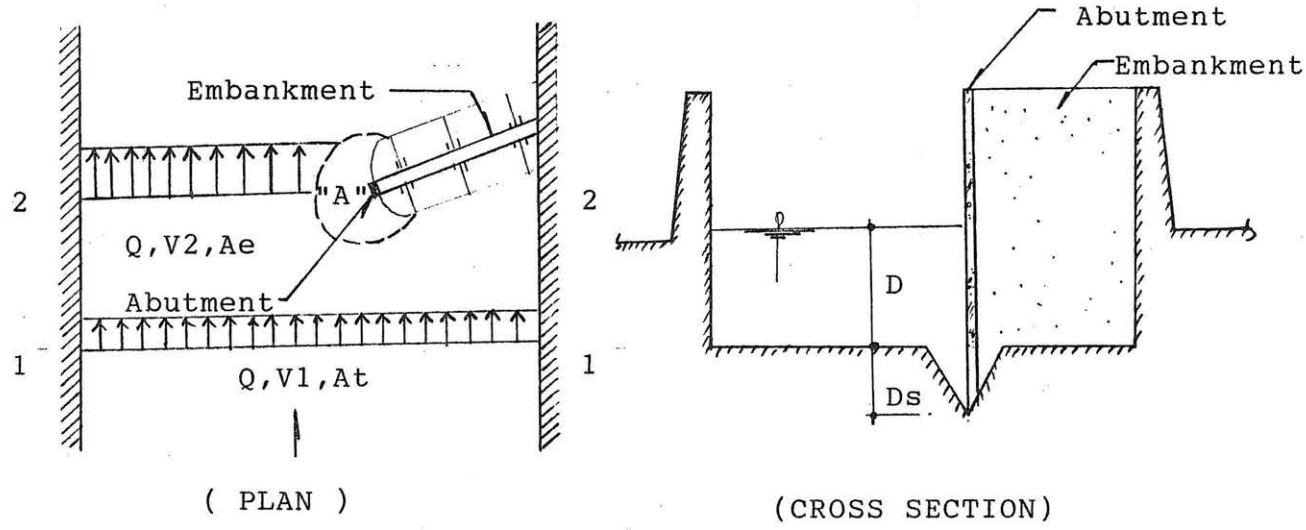

Fig.1 Definition Sketch for Abutment score

MECHANISM OF LOCAL SCOUR

Scour is the result of the interaction between the flow field,the obstacle,and the streambed. In order for the analysis to yield any insight into the general mechanism of scour,the analysis must begin with the predominant aspects of the flow.

The dominant feature of the flow in the neighborhood of the abutment is the large scale eddy structure,that is,the vortex systems which develop above the obstacle. This is basic mechanism of local scour. Depending on the type of obstacle and free stream conditions ,the eddy structure can be composed of any,all,none of three basic systems:the horseshoe vortex system,the wake vortex system,and the trailing vortex system.

Our interest in the large scale eddies makes it both convinient and natural to describe the flow field in terms of the vorticity.

$$\vec{\Omega} = \nabla \times \vec{V} = \xi i + \eta j + \zeta k \quad \text{..... (EQ. 1)}$$

where, $\vec{\Omega}$ is the vorticity vector and ξ, η, and ζ are its components in the i,j,and k directions respectively. The vorticity can be thought of as twice the average angular velocity of an infinitesimal fluid element.

If the pressure field induced by the abutment is sufficiently strong,it causes a three-dimensional separation of the boundary layer which,in turn,rolls up ahead of the abutment to form the horseshoe vortex system. It is important to note that no vorticity is created by the abutment in this instance,this is,the horseshoe vortex begins and ends on the channel bottom or walls.

Wake vortex system is generated by the obstacle itself contrary to the case of the horseshoe vortex. The wake vortex system is formed by the rolling up of the unstable shear layers generated at the surface of the obstacle. The strength of the vortices in the wake system varies greatly depending on obstacle shape and fluid velocity.

A streamlined obstacle will create a relatively weak while a bluff body produces a very strong one. The wake vortex system acts somewhat like a vacuum cleaner to pick up the bed material. It is then carried downstream by the eddies. Occasionally the literature will report the failure of a bridge due to deep scour downstream from the abutment. One reason for this type of failure is the wake vortex system.

The trailing vortex system usually occurs only on obstacles completely submerged in the fluid. It is composed of one or more discrete vortices attached to the top of the three dimensional obstacle and extending downstream. These vortices are formed when finite differences of pressure exist between two surfaces meeting at a corner such as at the top of the obstacle.

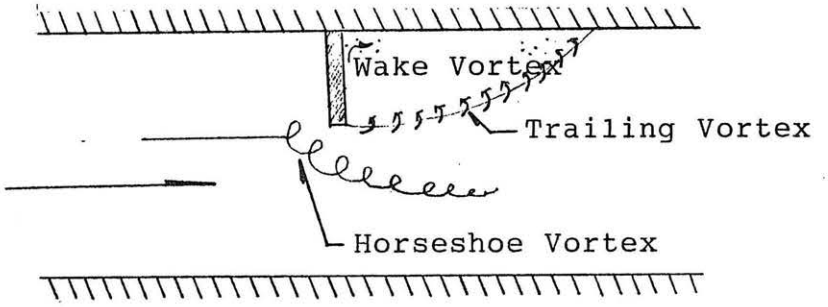

Fig.2 Formation of Vortices

DIMENSIONAL SCOUR DEVELOPMENT

1. Garde's Formula

R.J.Garde, K.Subramanya and K.D.Nambudripad(3) proposed a formula to calculate maximum scour depth based on dimensional development.

They considered that the variables entering the problem could be grouped into following four catagories.

1) Variables describing geometry of channel and of the abutment
   - the width of the channel : B
   - width of the abutment : b
   - angle of incidence : θ
2) Variables describing the flow
   - mean velocity : V
   - depth of flow : D
   - maximum scour depth : Ds
3) Variables describing the fluid
   - mass density of water : ρ
   - difference in specific weight between water and air : $\Delta\gamma$
   - dynamic viscosity : μ

4) Variables describing the sediment
- median size : d
- standard deviation : σ
  $<\sigma = 0.5(d84/d50 + d50/d16)>$
- difference in specific weight between sediment and water : $\Delta\gamma_s$

If the maximum scour depth relative to water surface is taken as the dependent variable

$$(D+Ds) = f(B,b,\theta,V,D,\rho,\Delta\gamma,\mu,d,\sigma,\Delta\gamma_s)$$

Because w(settling velocity of the sediment) is a function of d, ρ, μ, and $\Delta\gamma_s$, we can substitute w in place of μ.

$$(D+Ds) = f(B,b,\theta,V,D,\rho,\Delta\gamma,w,d,\sigma,\Delta\gamma_s)$$

Selecting V, D, and ρ, as a repeating variables yields

$$\frac{D+Ds}{D} = f\left(\frac{B}{D},\frac{b}{D},\theta,\frac{V}{\sqrt{\frac{\Delta\gamma}{\rho}D}},\frac{V}{w},\frac{d}{D},\sigma,\frac{V}{\sqrt{\frac{\Delta\gamma_s}{\rho}D}}\right)$$

Above equation can be repeated with some manipulations which is permissible within the theory of dimensional development.

$$\left(\frac{D+Ds}{D}\right) = f\left(\frac{B}{D},\frac{B-b}{B},\theta,\frac{V}{\sqrt{gD}},CD,\frac{d}{D},\sigma,\frac{\gamma_s}{\gamma}\right)$$

where, CD(average drag coefficient) $= \frac{4}{3}\frac{\Delta\gamma_s \cdot d}{w^2 \cdot \rho}$

Assuming that B/D, d/D and σ are of secondary importance, that effect of γ_s/γ is induced in CD, and that (B-b)/B is substituted as α, above equation can be reduced

$$\frac{D+Ds}{D} = f(\alpha,\theta,Fr,CD)$$

if θ is constant at 90°

$$\frac{D+Ds}{D} = f(\alpha,Fr,CD)$$

They considered CD as a constant through an experiment and showed the variation of (D+Ds)/D with Froude number, with α as the third variable.

$$\frac{D+Ds}{D} = c.Fr^{2/3} = k.\frac{1}{\alpha}.Fr^{2/3} \quad <\text{where, } k=f(CD)>$$

And they suggested k=4.0 for maximum scour depth

$$\frac{D+Ds}{D} = 4.0.\frac{1}{\alpha}.Fr^{2/3} \quad \text{.....(EQ.1)}$$

2. Froehlich's Formula

David C.Froehlich(2) suggested following equation based on the above dimensional development for clear water scour and live bed scour.

For clear water scour

$$\frac{Ds}{D} = 0.77.Ks.K_\theta\left(\frac{b}{D}\right)^{0.63} Fr^{1.19} \left(\frac{D}{d50}\right)^{0.44} \sigma_g^{-1.88} \quad \text{.....(EQ.2)}$$

and for live bed scour condition

$$\frac{Ds}{D} = 2.29.Ks.K_\theta\left(\frac{b}{D}\right)^{0.42} Fr^{0.61} \quad \text{.....(EQ.3)}$$

where, Ks=1.0 : for a vertical abutment with square or rounded corners.

Ks=0.82 : for a vertical abutment with wing walls and a sloped approach embankment.
Ks=0.55 : for a spill througt abutment and a sloped approach embankment
$K_\theta = (\theta/90)^{0.13}$

NON-DIMENSIONAL SCOUR DEVELOPMENT

1. Laursen's Formula

Emmett M.Laursen(5) considered local scour as a special case of scourin a long contraction.
From Fig.3

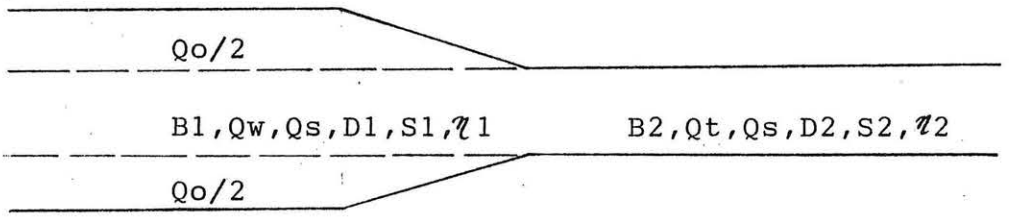

Fig.3 Definition sketch of a long contraction

Laursen developed an equation for at a contraction,where in addition to channel flow there is overbank flow concentrating into the contracted channel.

$$\frac{D2}{D1} = \left(\frac{Qt}{Qw}\right)^{6/7} \left(\frac{B1}{B2}\right)^{\frac{6(2+a)}{7(3+a)}} \left(\frac{\eta 2}{\eta 1}\right)^{\frac{6a}{7(3+a)}}$$

If Qt=Qw, $\eta 2 = \eta 1$, B1=1+2.75Ds, B2=2.75Ds and the depth of scour in the fictitious long contraction is y2-y1=1/11.5 Ds, the long contraction equation becomes

$$\frac{1}{D} = 2.75\,\frac{Ds}{D}\left[\left(\frac{1}{11.5}\,\frac{Ds}{D}+1\right)^{\frac{7(3+a)}{6(2+a)}} - 1\right]$$

through experiment, he suggested the value $\frac{7}{6}\,\frac{3+a}{2+a}$ is 1.70 in case bed shear stress τ_o is larger than critical shear stress τ_c

So, $$\frac{1}{D} = 2.75\,\frac{Ds}{D}\left[\left(\frac{1}{11.5}\,\frac{Ds}{D}+1\right)^{1.70} - 1\right] \quad \text{.....(EQ.4)}$$

where, $\frac{1}{D} = \frac{Qo.b}{Qw.D}$

Also, in case bed shear stress τ_o is less than critical shear stress τ_c

$$\frac{1}{D} = 2.75\,\frac{Ds}{D}\left[\left(\frac{1}{11.5}\,\frac{Ds}{D}+1\right)^{7/6}\left(\frac{\tau_o}{\tau_c}\right)^{1/2} - 1\right] \quad \text{.....(EQ.5)}$$

2. Liu's Formula

In 1961,Liu(3) suggested following formula based on the experiment.

$$\frac{Ds}{D} = K\left(\frac{b}{D}\right)^{0.40} Fr^{0.33} \quad \text{.....(EQ.6)}$$

where, b = effective length of the abutment
K = 2.15 : for vertical abutment
K = 1.1 : for spill slope embankment

3. Izzard's Formula

C.F.Izzard and J.N.Bradley(3) suggested an emperical formula.

$$D+Ds = 1.40\ q_1^{2/3} \quad \text{.....(EQ.7)}$$

where, $q_1 = q/\alpha$

$$\alpha = \frac{B-b}{B}$$

4. Zaghloul's Formula

N.A.Zaghloul and J.A.Mc Corquodale suggested an emperical formula.

$$\frac{Ds}{D} = 2.62\ Fr^{\frac{2}{3}}_1 \left(\frac{1}{\alpha}\right)\left(\frac{1}{\theta}\right)^{0.043}$$

where, α : opening ratio
θ : angle of inclination with respect to the main flow.

EFFECT OF ANGLE OF INCLINATION

Laursen and C.L.N.Sastry conducted experiments to study the effect of the angle of inclination of the abutment on maximum scour depth. Fig.4 shows that the results obtained by Sastry almost agree with those reported by Laursen(5),that is,for the inclined upstream (θ is less than 90°),the scour depth is more than for the inclined downstream. Other condition (such as flow characteristics,sediment size and opening ratio) remaining the same,the ratio of maximum to minimum scour can be as high as about 1.30 for different angles. Also, Laursen showed the shape of scour holes does not change with the angle of inclination as Fig.5.

The lateral extent of the scour hole is important in relation to the depth of scour. For an unrestricted scour hole at an abutment, the lateral extent along the line of the upstream face to the direction of flow can be taken as 2.75 times the depth of maximum scour . If the abutment is an angle to the direction of flow,the cross sectional lateral extents of the scour hole for 45,90,and 135° angle of incidence are showed in the Fig.6.

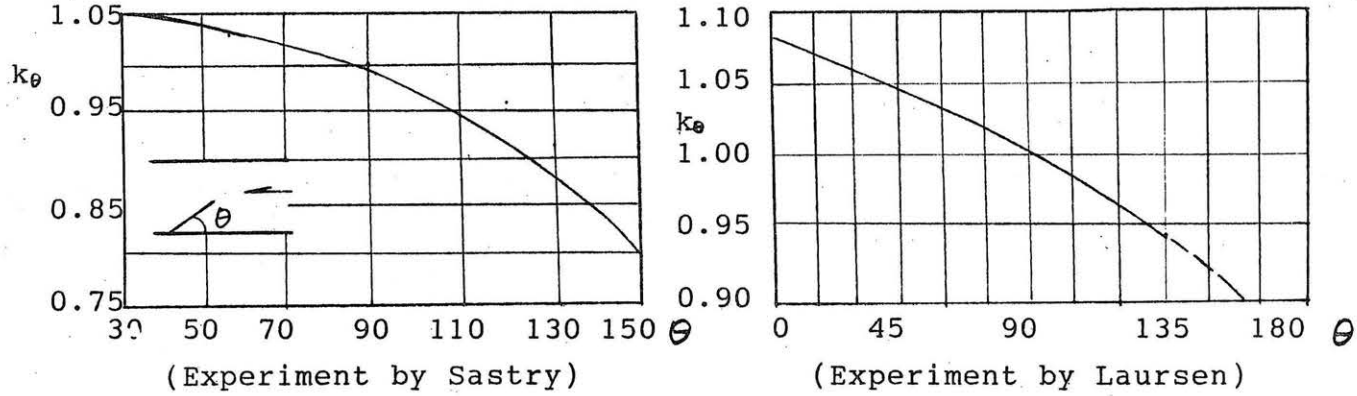

Fig.4 Effect of the Angle of Incidence on Scour Depth

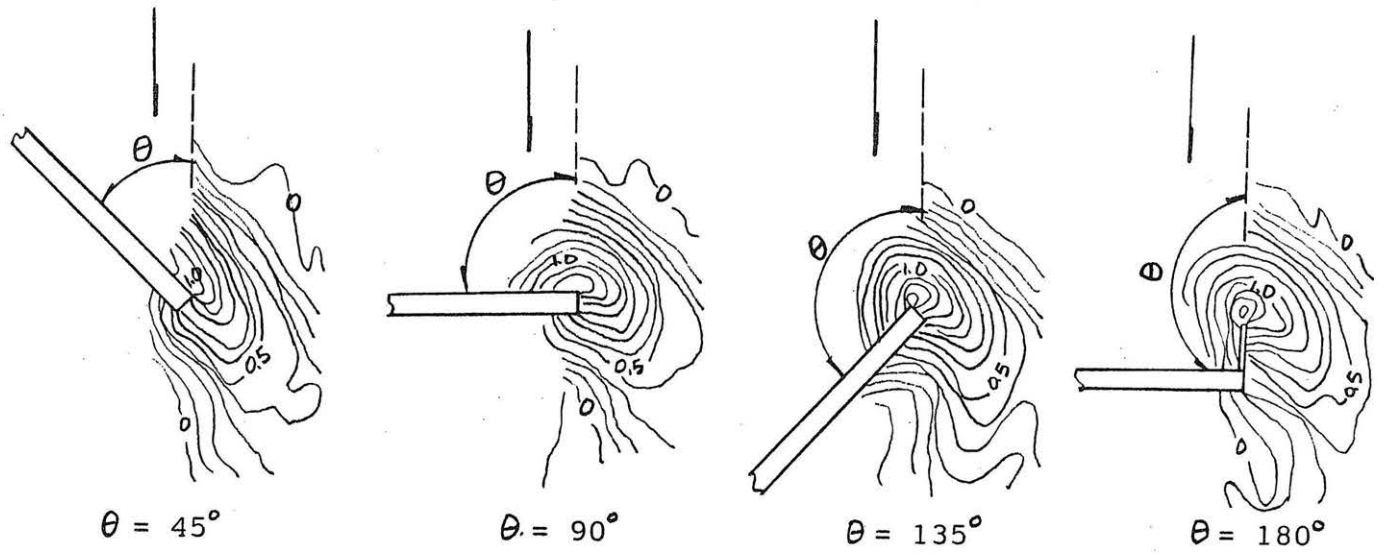

Fig.5 Patterns of Scour for Four Angles of Incidence

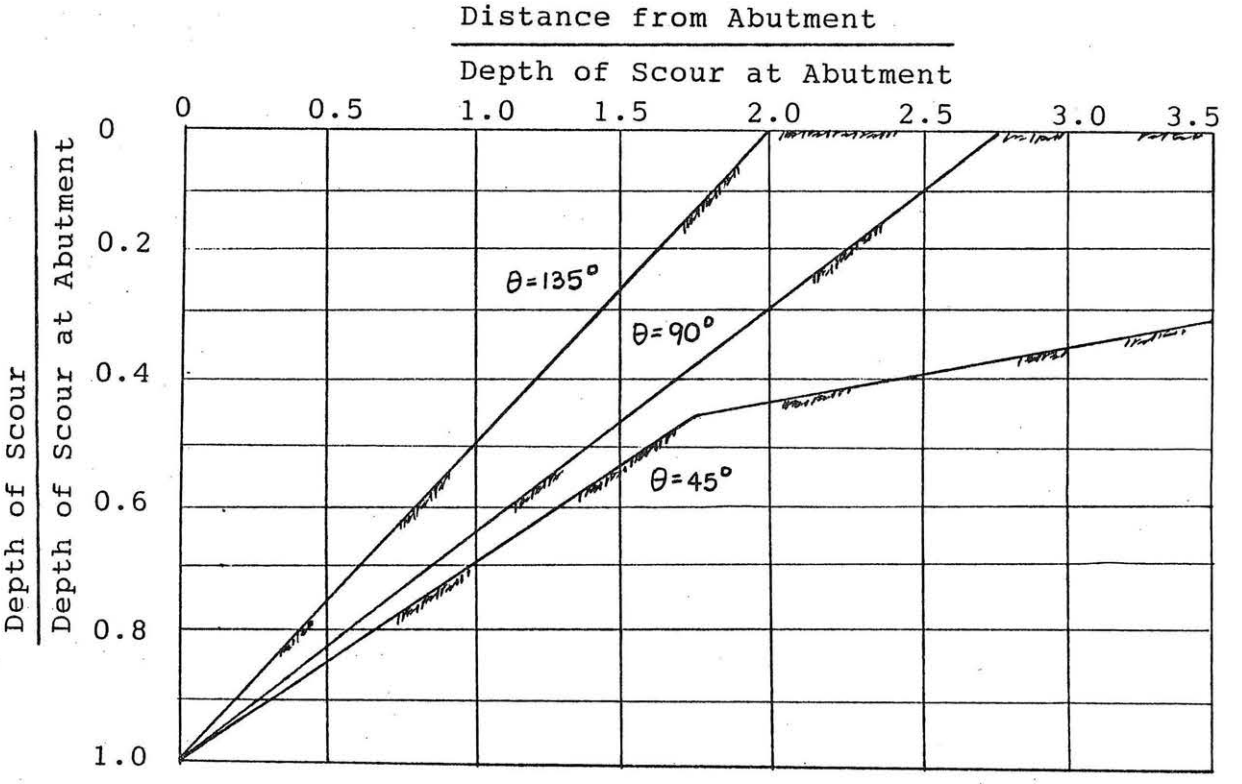

Fig.6 Lateral Influence of Scour Holes

APPLICATION TO DESIGN (CASE STUDY)

Because of difficulty in getting field data about abutment scour, one example in the IOWA Highway Research Board Bulletin No.8(7) was picked up as a case study for application to design.

1. Given Conditions
   - Flood discharge and depth

flood frequency	Qt(cfs)	Qw(cfs)	<Qt-Qw>/2(cfs)	D(ft)
25 years	18,500	17,500	500	5
50 years	26,500	24,000	1,250	6
100 years	35,800	30,800	2,500	7

   - The slope of the stream : 3ft/mile
   - Bed material : D=0.2 mm (w=6cm/sec)

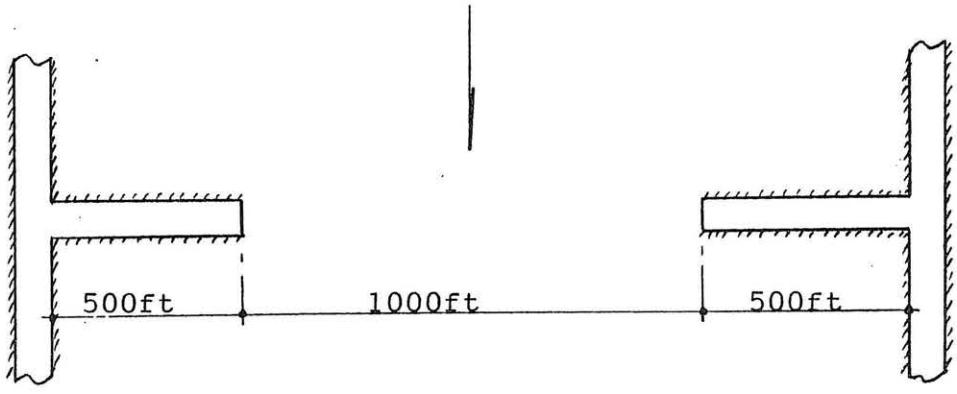

(PLAN)

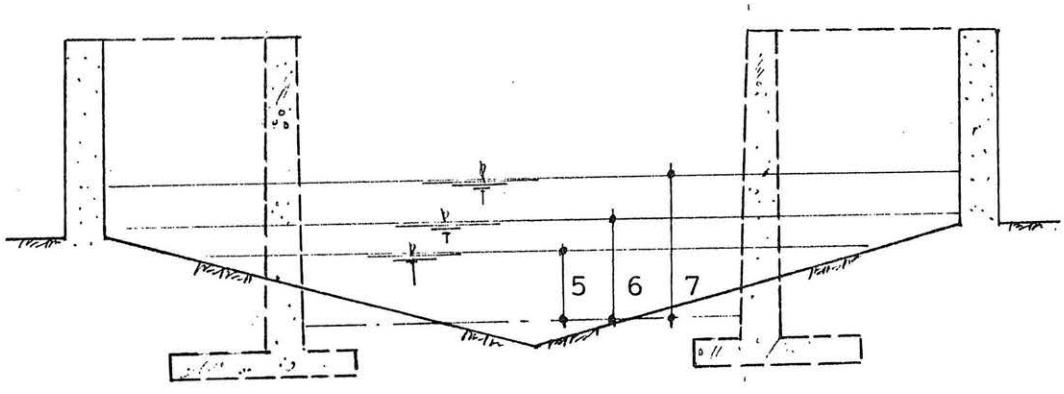

(SECTION)

Fig7. Sketch for Design Example

2. Summary of calculated maximum scour depth

No.	Formula	Unit	25years	50years	100years
1	Garde	ft	12.6	16.4	20.3
2	Froehlich	"	30.7	35.9	40.9
3-1	Laursen(For)	"	18.0	26.0	35.0
3-2	" (Fig)	"	23.4	34.8	48.0
4	Liu	"	23.1	26.5	29.7
5	Izzard	"	9.98	12.5	14.8
6	Zaghloul	"	9.50	12.1	14.7
Max.		"	30.7	35.9	48.0
Min.		"	9.50	12.1	14.7
Ave.		"	18.183	23.457	29.057
Max/Ave*100 %		%	168.8	153.0	165.2
Min/Ave*100 %		%	52.2	51.6	50.6

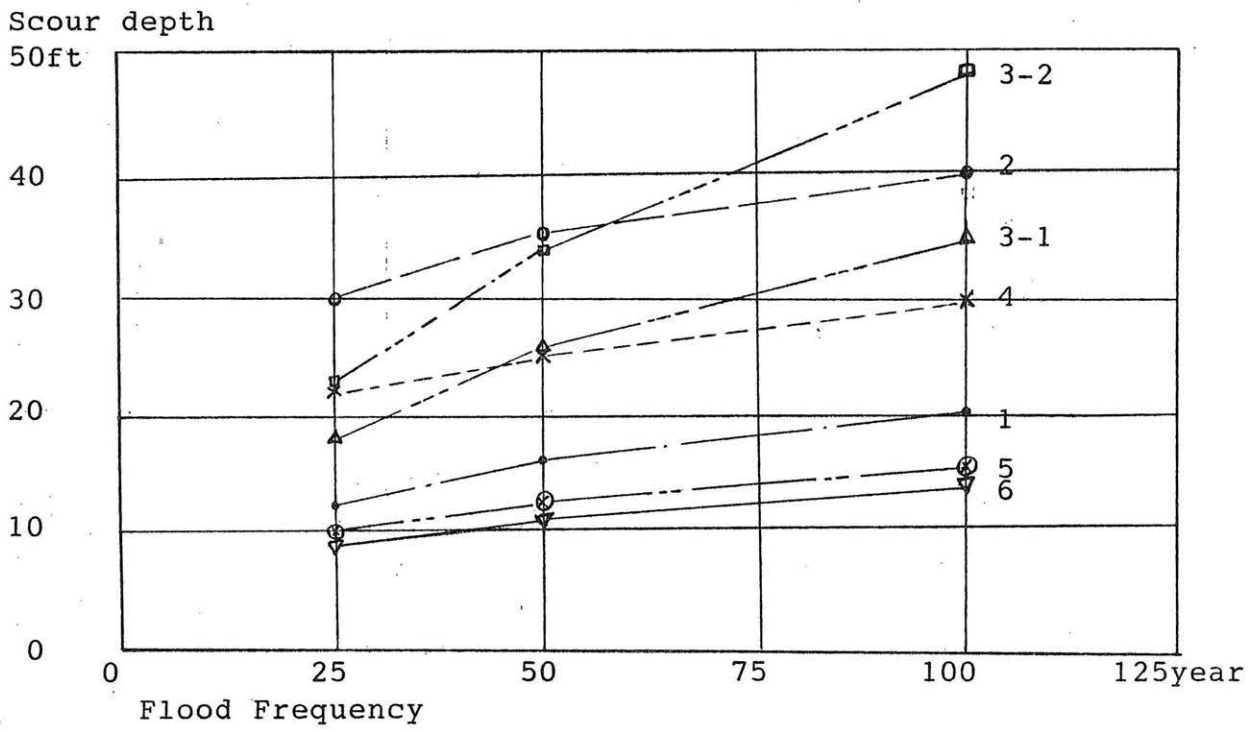

Fig.8 Comparison of Scour Depth

CONCLUSIONS

Through general research about local scour at abutment using literature review and quantitative comparison of local scour depth, the following conclusions can be drawn.

1) Maximum scour depth at abutment using formulae suggested by many investigators is not confined within narrow limits. So,the effort to get suitable formula for the applied natural channel condition is needed.

2) In the abutment scour Froude No. Fr. is a important factor. To get suitable Fr. at the head of the contraction by constructing abutments,the relationship between channel width,abutment width and upstream width between abutments should be studied.

3) Opening ratio by only channel width is not suitable. So,opening ratio should be defined by channel width and water depth.

4) The calculated results using Laursen's Formula and his suggested figures shows different value (Ref. summary of maximum scour depth). If Laursen's Formula is used to predict abutment scour depth, the correction factor should be considered.

5) Improvement of experimental equipments is required.For example, board is used instead of both abutment and embankment,but because most abutments consist of concrete structures and most embankments consist of earth structures,some different scour phenomena which don't match with real values is expected in the lavoratory.

REFERENCES

1. Ahman,Mushtaq,1953. Experiments on design and behavior of spur dikes. Proceedings,Minnesota International Hydraulics convention ,University of Minnesota,Minneapolis,Minnesota,pp 145-159.
2. Froehlich,David C.,1987. Abutment scour prediction(draft) U.S. Geological Survey,Verginia, pp1-21
3. Garde,R,J.,Subramanya,K. and Nambudripad,K.D.,1961. Study of scour around spur-dikes.Journal of the Hydraulics Division,ASCE, HY6, pp23-37.
4. Garde,R.J., Subramanya,K. and Nambudripad,K.D.,1963. Study of scour around spur-dikes. Journal of the Hydraulics Division,ASCE ,HY1, pp167-175
5. Laursen,Emmett M.1958. Scour at Bridge Crossings. Bulletin No.8 ,Iowa Highway Research Board,IOWA, pp1-53
6. Laursen,Emmett M.,1960. Scour at bridge crossings. Journal of the Hydraulics Division,ASCE,HY2, pp39-53
7. Laursen,Emmett M.,1970. Bridge design considering scour and risk . Transportation Engineeg Journal, PASCE,TE2, PP149-164
8. Laursen,Emmett M.,1980. Prediction scour at bridge and abutments . Engineering Experiment Station, College of Engineering,the university of Arizona,Tucson,Arizona, pp1-105
9. Mohammad,Akram Gill,1972. Erosion of sand beds around spur dikes . Journal of the Hydraulics Division,ASCE,Hy9, pp1587-1602
10. Richardson,E,V.,Simons,D.B,Julien,P,Y,1987. Highways in the river environment. U.S. Department of Transportation,Federal Highway Administration, pp v:75-86
11 Schneider,verne R.,1968. Mechanics of local scour. Dissertation , Colorado State University,Fort Collins,Colorado pp1-44
12 Shen,Hsieh Wen,Roper Alan T., Schneider Verne H.,1966.Analytical approach to local scour.International Association for Hydraulic Research,Colorado State University,Fort Collins Co. pp151-161.

LOCAL SCOUR AT BRIDGE PIERS

by Vincenza Cinzia Santoro

ABSTRACT: The general characteristics of local scour around cylindrical piers, an analysis of the parameters influencing the process, and a riview of predicting models are presented. A comparison among seven different equations, applied to some field data, is carried out. The results show a general trend to overestimate the scour depth, very often by very high factors. The spread of data for a constant value of pier width suggests that more knowledge about the influence of the other parameters is needed.

INTRODUCTION

In order to design the foundations of a bridge over an alluvial stream, it is necessary to know the lowest elevation of the stream bed which will occur during the anticipated life of the bridge in the vicinity of the piers and abutments. For a foundation design, a calculated risk must then be taken and the pier or abutment must be built in such a manner that the probability of scour action disturbing the stability of the structure is balanced against the replacement cost of the entire bridge structure. If means could be obtained for the prediction of the amount of scour, the calculated risk can then be confined to the probability of flood occurence.

This paper deals with the many different models suggested by researchers to predict local scour depth around bridge piers. An application of some of this equations to field data is presented, the main goal being to compare the relative magnitude of the predicted values to the measured ones.

DEFINITION AND CLASSIFICATION OF SCOUR

If an obstruction is placed in a stream, the flow pattern in the vicinity of that obstruction will be modified. Since the transport capacity is a function of the flow characteristics, the transport capacity pattern will also be modified. In any area where the transport capacity is not equal to the rate at which material is supplied, scour or deposition must occur.

Scour can then be defined as the enlargement of a flow section by the removal of material composing the boundary through the action of fluid in motion.

The total scour at a river crossing is composed of three components that, in general, are additive: general scour, due to long term changes in the river bed elevation (aggradation or degradation), which would occur whether an encroachment is present or not; contraction scour, resulting from the constriction of the waterway, either natural or due to the bridge and

its approaches; local scour, consequence of the interference with flow by piers or abutments, which accelerate the flow creating vortices that remove the material around them.

Local scour can occur in one of two ways.

Clear-water scour occurs when there is no movement of the bed material of the stream upstream of the crossing, but the acceleration of the flow and vortices created by the piers or abutments causes the material at their base to move. The bed shear stresses away from the scour area are thus equal to or less than the critical or threshold shear stress for the initiation of particle movement. The maximum scour depth is reached when the flow can no longer remove particles from the scour hole.

Live-bed scour (also referred to as scour with sediment transport) occurs when the bed material upstream of the crossing is also moving. Live-bed scour fluctuates, in response of passage of bed forms, about an equilibrium scour depth, which is reached when over a period of time the amount of material removed from the scour hole by the flow equals the amount of material supplied to the scour hole from upstream.

FLOW FIELD AROUND A PIER AND SCOUR PROCESS

The dominant feature of the flow near a pier is the large-scale eddy structure or the systems of vortices which develop around the pier. These vortex systems are the basic mechanism of local scour. Depending on the type of pier and free-stream conditions, the eddy structure can be composed of any, all or none of three basic systems: the horseshoe-vortex system, the wake-vortex system and/or the trailing-vortex system.

The approach flow goes to zero at the upstream face of the pier, in the vertical plane of simmetry, and since the approach flow velocity decreases from the free surface downward to zero at the bed, the stagnation pressure, also decreases. This downward pressure gradient drives the downflow. If the pressure field is sufficiently strong, it causes a three-dimensional separation of the boundary layer, which rolls up ahead of the pier to form the horseshoe-vortex system.

The stagnation pressure causes not only downflow, but also sidewards acceleration of flow past the pier. The separation of flow at the sides creates the wake-vortices at the interfaces to the main stream. These vortices are translated downstream with the flow and interact with the horseshoe-vortex at the bed causing it to oscillate laterally and vertically. They also act as little tornados lifting sediment from the bed.

The trailing-vortex system usually occurs only on completely submerged piers and is composed of one or more discrete vortices attached to the top of the pier and extending downstream.

Finally, a bow wave develops at the surface with rotation in the opposite sense to that in the horseshoe-vortex. The bow wave becomes important in relatively shallow flows where it interferes with the approach flow and causes a reduction in the strenght of the downflow.

Fig. 1 shows the flow pattern at a cylindrical pier.

Some general characteristics are common to all the scour patterns around a pier. The upstream portion of the hole has the approximate form of an inverted cone, with side slopes equal to the angle of repose of the bed material. Deposition which occurs in the low velocity area behind the pier divides the downstream portion of the scour hole into two separate tails.

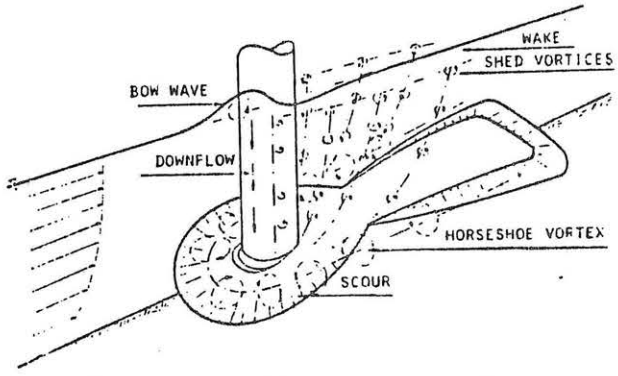

FIG. 1 - Diagrammatic flow pattern at a cylindrical pier.

ANALYSIS AND INFLUENCE OF SCOURING PARAMETERS

The many parameters which influence scour around bridge piers can be arranged into four groups:
1. fluid variables: density of fluid, kinematic viscosity of fluid;
2. stream flow variables: depth of approach flow, mean velocity of undisturbed flow, roughness of the approach flow;
3. stream bed materials: grain diameter and form, grain size distribution, density of the sediment, cohesive properties;
4. bridge piers variables: pier dimensions, pier shape, surface roughness, number or spacing of the piers, orientation of piers to approach flow direction, pier protection.

Because of the complexities and costs of measuring, analyzing and evaluating all of the above mentioned variables, many investigators assume some restrictive conditions:
- the differences between the laboratory and field values for density, viscosity and acceleration due to gravity can be neglected;
- channels can be considered sufficiently wide so that the bridge pier does not cause a significant contraction;
- alluvial non-cohesive (often uniform) particle-sized bed material;
- perfectly smooth piers without scour protection systems, such as riprap.

These assumpions and restrictions reduce the list of variables to the following:
1. fluid density, kinematic viscosity of the fluid;
2. sediment diameter, bed sediment density;
3. approach flow depth, mean velocity of the undisturbed flow;
4. pier width, pier shape, orientation of the pier.

There are several references in the literature stating that the scour depth is affected by the flow depth relative to the pier size. In particular, from the experimental results it may be concluded that for y/b >3 the influence of this parameter can be neglected and that at shallow flow depths the scour depth increases with depth of flow.

The volume of the conical local scour hole formed around the upstream half of the perimeter of the pier is proportional to the cube of the projected width of the pier. The larger is the pier, the larger is the scour volume and the longer is the time required to erode it at a given shear stress.

For the case of clear-water scour, the scour depth increases almost linearly with velocity. The limiting scour depth is approached slowly. For scour with sediment motion Melville (1984) obtained a generalized scour depth versus flow velocity relationship, based upon the results of laboratory studies, that shows scour maxima at both the thereshold condition and the transition flat bed condition of bed motion.

For clear-water scour, the equilibrium depth is not affected by particle size as long as $b/D_{50}>25$. For smaller values the erosion process is impeded and the scour depth decreases. For the case of scour with sediment motion, Laursen and Toch (1953) stated that, for uniform size sand, since the sediment size will not have any effect on any existing balance of the transport capacities, the equilibrium depth of scour should not be affected by a change in sediment size.

Raudkivi and Ettema (1977) stated that sediment grading has a strong influence on the equilibrium depth of clear-water scour and presented a relationship between the maximum clear-water scour depth and the geometric standard deviation of sediment grading. The effect of sediment grading on the depth of live-bed scour is considerably more complex.

Piers can be classified in two categories: blunt-nosed, where a strong horseshoe-vortex system and thus the maximum scour depth occur at the pier nose, and sharp-nosed, where the horseshoe-vortex system is very weak and the maximum scour depth occurs near the downstream end. Laursen found that the shape coefficient, defined as the ratio between scour depth of a particular shape to that of the rectangular shape, varies with the shape of the pier in such a way that the best that can be expected is a 30% reduction, and simple round pier has only 10% of reduction. Moreover, it must be taken in account that, if the pier is not perfectly aligned with the flow, the effect of shape may be entirely lost.

For pier shapes other than circular, the depth of local scour depends on the alignment of the pier with flow. The local scour depth is related to the projected width of the pier, and this width increases with the angle of attack of flow. With an increasing angle of attack, the location of maximum scour depth moves along the exposed side of the pier from the front to the rear end of the pier. Some authors have proposed the use of the projected width in their formulas, but this gives an overestimate in most cases.

Some authors have carried out experiments with various bed material densities under identical conditions. The conclusion was that the scour depth increases with decreasing bed material density.

DESCRIPTION OF MODELS

A number of equations for predicting scour were proposed by a number of researchers over the past century. A list of formulae developed to predict the anticipated depth of local scour at intermediate bridge piers follows.

The Inglis-Poona equation (1938)

$$\frac{d_s}{b} = 1.70 \left(\frac{q^{2/3}}{b} \right)^{0.78} \quad (1)$$

is based on a series of model tests run without general movement of the bed. The use of the discharge per unit width in the contraction would seem to imply greater scour at the piers if more piers were placed in the cross-section. This contraction effect might be actually the velocity effect for clear-water scour.

Chitale's formula (1944)

$$\frac{d_s}{y} = 6.65\, Fr - 0.51 - 5.49\, Fr^2 \quad (2)$$

is based on the results of an extension of the original Poona model tests. Most of the tests were for the case of clear-water scour, but for some where there was coarse sand laid around the pier, the finer sand from upstream moved down to the scoured area.

The Inglis-Lacey relationship (1949)

$$d_s = 0.946 \left(\frac{Q}{f}\right)^{1/3} - y \quad (3)$$

is a statement that the depth of scour measured from the water surface is twice the Lacey regime depth. The principal restriction of this relationship is that of regime channel. However, it also ignores the pier size, shape and alignment.

Blench's equation (1957)

$$\frac{y + d_s}{y_r} = 1.8 \left(\frac{b}{y_r}\right)^{1/4} \quad (4)$$

can be obtained from the Inglis-Poona equation if the exponent 0.78 is changed to 0.75. The limitation of the Poona equation therefore still apply, plus a contradiction because the conditions of the Poona tests were those of

clear-water scour and regime theory implies a low to moderate rate of sediment movement.

The Laursen relationship (1960)

$$\frac{b}{y} = 5.5 \frac{d_s}{y} \left[\left(\frac{d_s}{11.5 y} + 1 \right)^{1.7} - 1 \right] \quad \text{.....(5)}$$

was based on an analysis adapting the solution of the long contraction, with a balance of sediment transport capacity in the normal and contracted sections, to the pier. It is valid for subcritical flow with a goodly rate of sediment movement. A second relationship

$$\frac{b}{y} = 5.5 \frac{d_s}{y} \left[\left(\frac{d_s}{11.5 y} + 1 \right)^{7/6} / \left(\tau_o / \tau_c \right)^{1/2} - 1 \right] \quad \text{.....(6)}$$

where $\tau_o/\tau_c = V^2/120\ D^{2/3}\ y^{1/3}$, was similarly adapted from an analysis of long contraction in which the contraction scoured to give a boundary shear equal to the critical tractive force for the bed material and the shear in the approach was less than this value.

Ahmad formula (1962)

$$d_s = K\ q^{2/3} - y \quad \text{.....(7)}$$

in which K is a multiplying factor that varies from 1.3 to 2.3 according to the general situation of the bridge and other conditions, is based on field experience and model studies. It was derived for bridges crossing alluvial rivers in deep sand fills.

Larras (1963) found that

$$d_{se} = 1.42\ K\ b^{0.75} \quad \text{.....(9)}$$

in which K is a coefficient depending on pier shape. It is suggested to be equal to 1 for circular piers and to 1.4 for rectangular piers aligned with the flow. The equation was obtained collecting available scour data from various rivers, after a flood had passed.

Neill's equation (1964)

$$\frac{d_s}{b} = 1.5 \left(\frac{y}{b} \right)^{0.3} \quad \text{.....(8)}$$

is based on model study data and is supposedly the maximum scour that can occur at any velocity. For round-nosed piers the coefficient should be changed to 1.2. For oblique piers the width is taken as the projected width and the coefficient 1.5 is used for all the non-aligned shapes. Neill's

equation is almost exactly the first Laursen and Toch graphic relationship (1956), drawn by eye on a simple plot.

Blench (1962) converted the original Inglis-Poona equation to

$$\frac{y_r + d_s}{y_r} = 1.8 \left(\frac{b}{y_r}\right)^{1/4} \quad \text{.....(10)}$$

and Arunachalam (1965) did the same obtaining

$$\frac{y_r + d_s}{y_r} = 1.95 \left(\frac{b}{y_r}\right)^{1/6} \quad \text{.....(11)}$$

Breusers (1964) proposed

$$d_{se} = 1.4\ b \quad \text{.....(12)}$$

for scour with continuous sediment motion and circular piers.

Hancu (1965) gave experimental results for circular piers, obtaining

$$\frac{d_s}{b} = 3.3 \left(\frac{d}{b}\right)^{0.2} \left(\frac{y}{b}\right)^{0.13} \quad \text{.....(13)}$$

for natural sands.

Shen's equations

$$\frac{d_{se}}{b} = 11.0\ Fr^2 \quad \text{.....(14)}$$

$$\frac{d_{se}}{b} = 3.4\ Fr^{0.67} \quad \text{.....(15)}$$

are based on model studies conducted at CSU and other measurements, and are for the limiting case of clear-water scour. There is a velocity effect but not a sediment size effect.

Shen, Schneider and Karaki (1966) stated that the equilibrium depth of scour should be functionally related to the pier Reynolds number. Some experimental work was done with circular piers. From these results and others from literature a relation was derived

$$d_{se} = 0.00073\ Re^{0.619} \quad \text{.....(16)}$$

The equation was tested also with other data, with pier shape different than the circular. If dunes are present on the bed at the design velocity, it is suggested to add one half the expected hight of these dunes to the estimated equilibrium depth of scour to get the maximum probable depth.

Coleman (1971) analysed some data and results from experiments on circular piers in sand under conditions of continuous sediment transport. The correlation obtained was

$$\frac{d_s}{b} = 1.49 \left(\frac{V^2}{gy}\right)^{0.1} \quad \text{.....(17)}$$

A prediction equation was developed at CSU (1975) for equilibrium scour depth

$$\frac{d_{se}}{y} = 2.0 \left(\frac{b}{y}\right)^{0.65} Fr^{0.43} \quad \text{.....(18)}$$

The coefficient is equal to 2.2 for square-nosed piers. The exponents were derived from laboratory data.

Basak, Basamily and Ergun (1975) performed tests with square piers in coarse sand. The water depths were small and for most of the tests $V>V_c$, but as both depth and velocity were varied simultaneously no independent variation of parameters was obtained. The results were correlated with the equation

$$d_s = 0.558\ b^{0.586} \quad \text{.....(19)}$$

for varying y, which can be interpreted only as a decrease of ds/b with increasing b/y.

Jain (1981) formulated the equation

$$\frac{d_s}{b} = 1.84 \left(\frac{y}{b}\right)^{0.30} (Fr_c)^{0.25} \quad \text{.....(20)}$$

valid for clear water scour around cylindrical piers, which is very similar to that of Laursen and Toch but includes the effect of sediment size on scour depth.

Baker (1981), after a study of the mechanism of the vortex in the scour hole, for $V/V_c<1$, arrived to a formula which adjusted with experimental results, is

$$\frac{d_s}{b} = [g_1 \frac{V}{V_c}][k_1 \tanh(k_{2b} \frac{y}{})][g_2 g_3] \quad \text{.....(21)}$$

in which k_1 and k_2 are functions of $G=(\rho_s - \rho)gD^3/(\rho v^2)$; g_1 is a function of V/V_c; g_2 and g_3 are function of shape and incidence to the flow.

Raudkivi and Ettema (1977,1983) found that the maximum depth of clear-water scour, for a cylindrical pier in a uniform grain-size sediment,

with a scour process unaffected by relative flow depth or relative grain size, is

$$\frac{d_{se}}{y} = 2.3 \quad \text{.....(22)}$$

For non-uniform sediment, this equation becomes

$$\frac{d_{se}}{y} = 2.3\ K_{\sigma} \quad \text{.....(23)}$$

where K_{σ} is a coefficient whose value is a function of σ_g.

Froehlich (1987) used multiple-linear-regression analysis to develop a prediction equation for local live-bed scour

$$\frac{d_s}{b'} = 0.32\ \Phi \left(\frac{b'}{b}\right)^{0.62} \left(\frac{y}{b}\right)^{0.46} Fr^{0.20} \left(\frac{b}{D}\right)^{0.08} \quad \text{.....(24)}$$

in which $b' = b \cos\alpha + l \sin\alpha$ is the pier width projected normal to the approach flow and Φ is 1.3 for a square-nosed pier, 1.0 for a round-nosed pier and 0.7 for a sharp-nosed pier.

SELECTION OF MODELS AND APPLICATION TO FIELD DATA

Froehlich (1987) collected and analysed existing field measurements of local scour at bridge piers.

Seven models were selected and applied to those data: Laursen (Eq. 5); Neill (Eq. 8); Larras (Eq. 9); Breusers (Eq. 12); Shen, Schneider and Karaki (Eq. 16); CSU (Eq. 18); Froehlich (Eq. 24).

The results are shown in Figs. 2-8, where the ratio between the calculated and the measured depths of scour is plotted against the pier width.

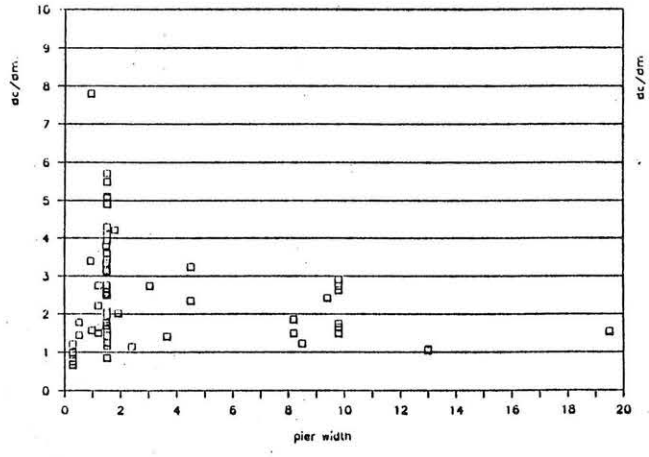

FIG. 2. - Laursen equation

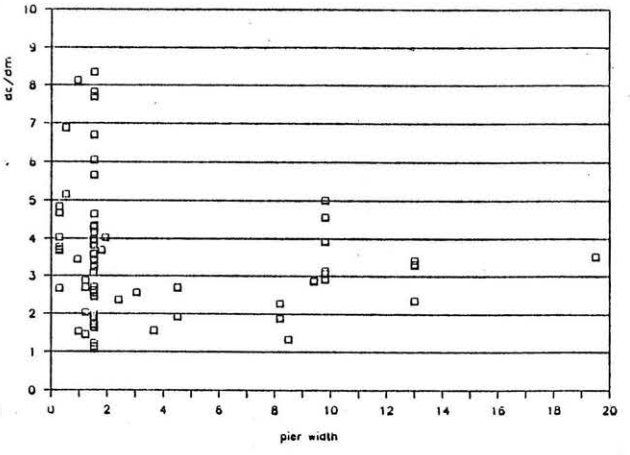

FIG. 3. - Neill equation

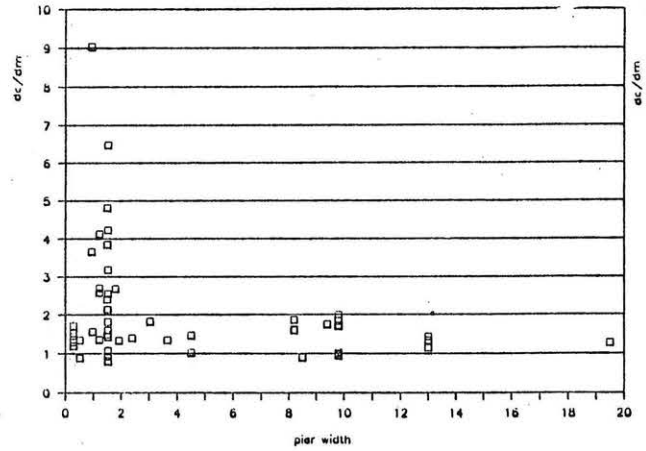

FIG. 4. - Larras equation

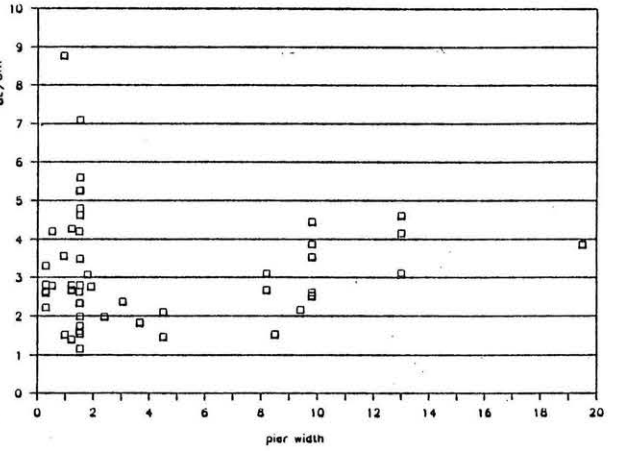

FIG. 5. - Breusers equation

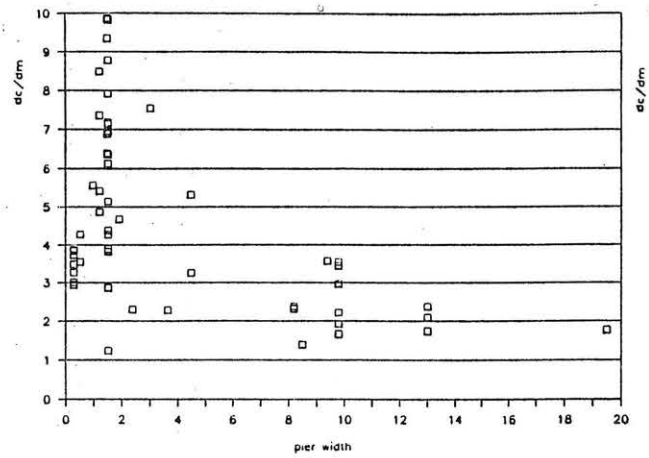

FIG. 6. - Shen, Schneider and Karaki equation

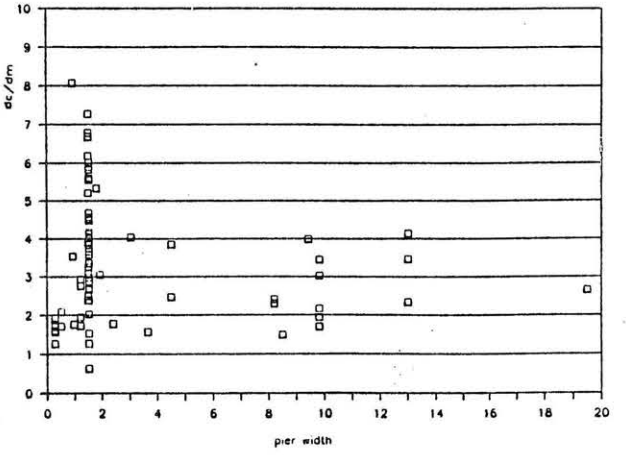

FIG. 7. - CSU equation

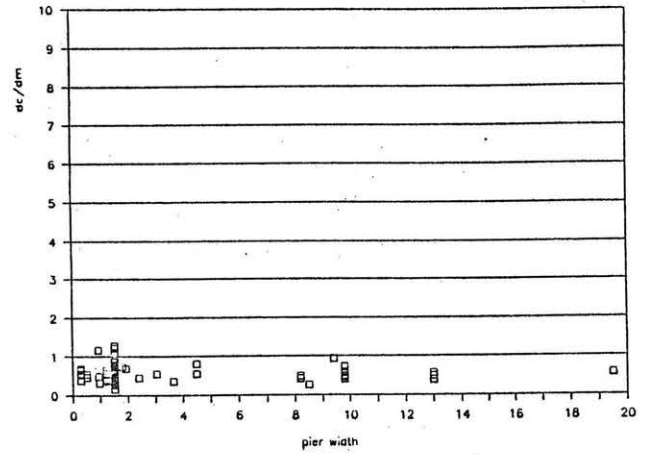

FIG. 8. - Froehlich equation

COMPARISON AND RESULTS

The data look quite spread in all the graphs.

There are some remarks that can be made.

The adopted selection of the parameters in abscissa (pier width) and ordinate (calculated depth/measured depth) doesn't allow a comparison on the effect of different parameters (velocity, sediment size, sediment gradation, flow depth) on scour depth; nevertheless the available data refer to very different conditions. For example, the bed sediment mean diameter varies from 0.008 to 90 mm; some bed material was graded and some was not; the angle of attack varied between 0° and 35°. However all the mearurements were referred to subcritical flow, the higher value of the Froude number being 0.86.

A slightly better set of predicted values was given by Larras' formula.

Froehlich's equation was the only one that seems, in general, to underestimate the scour depth.

All the equations give highly different results for the same pier width (and this is particularly evident for b=1.52, for which many data are available). This suggest that the weight of the other parameters must be important and not yet well considered in any of the equations.

CONCLUSION

Although a good knowledge of the qualitative aspects of the scouring phenomenon has been reached during the last fifty years of research activity, a complete quantitative understanding is still far.

As the depth of scour is influenced by very many parameters, it is difficult to try to take all of them in account, their influence being not easily comprehensible both with a theoretical approach and an experimental approach.

In particular, the results show that, while the effect of pier width is fairly well taken in account (or at least approximately in the same way for the used models), the influence of the other parameters should be better analyzed, like the scattering of the points with the same value of pier width suggests.

APPENDIX I. - REFERENCES

1. Arizona Department of Transportation, Federal Highway Administration, "A Study of Selected Waterway Bridges in Arizona with Potential Scour related Foundation Problems", 1979.
2. Baker, C.J. "New Design Equations for Scour around Bridge Piers" Journal of the Hydraulics Division, ASCE, Vol. 107, 1981, pp. 507-511.
3. Blaisdell, F.W., Anderson, C.L., Hebaus, G.G., "Ultimate Dimensions of

Local Scour", Journal of the Hydraulics Division, ASCE, Vol. 107, 1981, pp. 327-337.
4. Breusers, H.N.C., Nicollet, G., Shen, H.W., "Local Scour around Cylindrical Piers", Journal of Hydraulic Research, 1977, pp. 211-252.
5. Carstens, M.R., "Similarity Laws for Localized Scour", Journal of the Hydraulics Division, ASCE, 1966, pp. 13-36.
6. Copp, H.D., Johnson, J.P., Mc Intosh, J.L., "Prediction Methods for Determination of Anticipated Depths of Local Pier Scour", 1987.
7. Froehlich, D.C., "Local Scour at Bridge Piers from Onsite Measurements", U.S. Geological Survey, Water Resources Division, 1987.
8. Jain, S.C., "Maximum Clear-Water Scour around Circular Piers", Journal of Hydraulic Engineering, ASCE, Vol. 109, 1981, pp.611-626.
9. Lane, E.W., Borland, W.M., "River Bed Scour during Floods", Transactions ASCE, Vol. 119, 1954, pp. 1069-1089.
10. Laursen, E. M., "Observation on the Nature of Scour", Proceedings 5th Hydraulics Conference, State University of Iowa, Iowa, 1952, pp. 179-197.
11. Laursen, E.M., "Model-Prototype Comparison of Bridge Pier Scour"
12. Laursen, E.M., "Scour at Bridge Crossings", Transaction ASCE, Vol. 127, 1962, pp. 166-209.
13. Laursen, E.M., "Bridge Design considering Scour and Risk", Transportation Engineering Journal, ASCE, 1970, pp.149-164.
14. Laursen, E.M., "Predicting Scour at Bridge Piers and Abutments", General Report no. 3, University of Arizona, 1980.
15. Laursen, E.M., "Assessing Vulnerability of Bridges to Floods", Transportation Research Record 950, 1983, pp. 222-229.
16. Laursen, E.M., "Prediction of Scour in River Engineering"
17. Laursen, E.M., Toch, A., "Model Studies of Scour around Bridge Piers and Abutments - Second Progress Report", Proceedings 31st Annual Meeting Highway Research Board, 1952.
18. Laursen, E.M., Toch, A., "A Generalized Model Study of Scour around Bridge Piers and Abutments", Proceedings Minnesota International Hydraulics Convention, 1953, pp. 123-131.
19. Laursen, E.M., Toch, A., "Scour around Bridge Piers and Abutments", Bulletin no. 4, Iowa Highway Research Board, 1956.
20. Melville, B.W., "Live-Bed Scour at Bridge Piers", Journal of Hydraulic Engineering, ASCE, Vol. 110, 1984, pp. 1234-1247.
21. Melville, B.W., Raudkivi, A.J., "Flow Characteristics in Local Scour at Bridge Piers", Journal of Hydraulic Research, 1977, pp. 373-380.
22. Raudkivi, A.J., "Functional Trends of Scour at Bridge Piers", Journal of Hydraulic Engineering, ASCE, Vol.112, 1986, pp.1-13.
23. Raudkivi, A.J., Ettema, R., "Effect of Sediment Gradation on Clear-Water Scour", Journal of the Hydraulics Division, ASCE, Vol. 103, 1977, pp. 1209-1213.
24. Raudkivi, A.J., Ettema, R., "Clear-Water Scour at Cylindrical Piers", Journal of Hydraulic Engineering, ASCE, Vol. 109, 1983, pp. 338-350.
25. Raudkivi, A.J., Ettema, R., "Scour at Cylindrical Bridge Piers in

Armored Beds", Journal of Hydraulic Engineering, ASCE, Vol. 111, 1985, pp. 713-731.
26. Richardson, E.V., "Scour at Bridges", FHWA Technical Advisory (draft), 1987.
27. Richardson, E.V., Simons, D.B., Julien, P.Y., "Highways in the River Environment", U.S. Department of Transportation, Federal Highway Administration, 1987.
28. Roper, A.T., Schneider, V.R., Shen, H.W., "Analytical Approach to Local Scour", Proceedings XII Congress of IAHR, Fort Collins, Colorado, 1967.
29. Shen, H.W., Schneider, V.R., Karaki, S., "Local Scour around Bridge Piers", Journal of the Hydraulics Division, ASCE, 1969, pp. 1919-1940.
30. Stevens, M.A., "Scour at Bridge Piers", Lecture Notes, Boulder, Colorado, 1987.
31. Structures Section Bridge Scour Committee, Highways Division, Arizona Department of Transportation, "Countermeasures against Scour at Selected Waterway Bridges in Arizona with Potential Scour related Foundation Problems", 1981.
32. Tanaka, S., Yano, M., "Local Scour around a Circular Cylinder", Proceedings XII Congress of IAHR, Fort Collins, Colorado, 1967.

APPENDIX II. - NOTATION

The following symbols are used in this paper:

b = pier width;
d_s = depth of scour below mean bed level;
d_{se} = equilibrium scour depth below mean bed level;
d_{sm} = maximum equilibrium scour depth below mean bed level;
D_{50} = mean sediment size;
f = friction factor;
Fr = Froude noumber;
Fr_c = critical Froude noumber;
g = gravitational acceleration;
l = lenght of the pier;
q = discharge per unit width;
Q = total discharge;
Re = pier Reynolds noumber;
V = mean approach flow velocity;
V_c = mean approach flow critical velocity;
y = upstream flow depth;
y_r = regime depth;
α = angle of attack of the flow;
ν = kinematic viscosity of the water;

ρ = water density;
ρ_s = bed material density;
σ_g = geometric standard deviation of particle size distribution;
τ_c = critical shear stress;
τ = bed shear stress.